Developmental Biology
Stem Cells and Regenerative Medicine

Single Cell Transcriptomics-Informed Induced Pluripotent Stem Cells Differentiation to Tenogenic Lineage

Reviewed Preprint
v2 • November 5, 2024
Revised by authors

Reviewed Preprint
v1 • November 8, 2023

Angela Papalamprou, Victoria Yu, Wensen Jiang, Julia Sheyn, Tina Stefanovic, Angel Chen, Chloe Castaneda, Melissa Chavez, Dmitriy Sheyn

Orthopaedic Stem Cell Research Laboratory, Cedars-Sinai Medical Center, Los Angeles, United States • Board of Governors Regenerative Medicine Institute, Cedars-Sinai Medical Center, Los Angeles, United States • Department of Biomedical Sciences, Cedars-Sinai Medical Center, Los Angeles, United States • Department of Orthopedics, Cedars-Sinai Medical Center, Los Angeles, United States • Department of Surgery, Cedars-Sinai Medical Center, Los Angeles, United States

eLife Assessment

The authors established a **useful** syndetome differentiation protocol from human induced pluripotent stem cells, guided by single-cell transcriptomic analysis. Their findings could significantly impact the field, particularly for patients needing tendon cell therapy. However, the evidence presented is currently **incomplete**, as the authors did not yet test the applicability of their protocol across multiple human induced pluripotent stem cell lines.

https://doi.org/10.7554/eLife.89652.2.sa4

Abstract

Summary

During vertebrate embryogenesis, axial tendons develop from the paraxial mesoderm and differentiate through specific developmental stages to reach the syndetome stage. While the main roles of signaling pathways in the earlier stages of the differentiation have been well established, pathway nuances in syndetome specification from the sclerotome stage have yet to be explored. Here, we show stepwise differentiation of human iPSCs to the syndetome stage using chemically defined media and small molecules that were modified based on single cell RNA-sequencing and pathway analysis. We identified a significant population of branching off-target cells differentiating towards a neural phenotype overexpressing Wnt. Further transcriptomics post-addition of a WNT inhibitor at the somite stage and onwards revealed not only total removal of the neural off-target cells, but also increased syndetome induction efficiency. Fine-tuning tendon differentiation *in vitro* is essential to address the current challenges in developing a successful cell-based tendon therapy.

Introduction

Tendons are necessary to support body movement by transferring forces between muscle and bone. Unfortunately, tendon injuries are quite prevalent in athletes and in the aging population, comprising 45% of musculoskeletal consultations in the US alone.[1] Tendons are structurally complex tissues, and their low vascularity and cellularity are contributing factors to their poor regenerative capacity.[2] The current standard of treatments for severe tendon injury includes conservative approaches and/or surgical intervention.[1] However, the resulting prolonged rehabilitation, muscle weakness, and high re-injury rates dramatically limit patient outcomes.[3] Development of a stem cell-mediated solution could improve patient outcomes, yet current approaches fall short in terms of tissue biomechanical performance and tissue organization.[4–6]

Cell-based therapies have shown potential for tendon repair.[7] Autologous tendon progenitors and Mesenchymal Stromal Cells (MSCs) have been explored as potential cell sources, however, their limitations for clinical application are associated with their heterogeneity and the need for *in vitro* expansion for obtaining clinically relevant cell numbers. Cell expansion *in vitro* can result in phenotypic drift and subsequent functional loss, in addition to low proliferative ability.[8] Utilizing tenocytes differentiated from induced pluripotent stem cells (iPSCs) holds promise due to their unparalleled developmental plasticity, unlimited self-renewal capacity, and the potential scalability for an off-the-shelf cell source application. Well-established protocols have been developed for the differentiation from pluripotent stem cells to different musculoskeletal cell types including chondrocytes and osteoblasts.[9–12] Recent studies have successfully differentiated tenocytes using mouse iPSCs and Embryonic Stem Cells.[13–16] Though, recent work has shown a divergence in developmental processes between mouse and human embryos and subsequent differences in developmental cues on tenogenic differentiation between species.[17–20] This highlights the importance of researching the developmental cues of human cells. Furthermore, other studies have either not reported induction efficiency or showed limited syndetome-like/tenocyte induction.[13,21] Deriving a homogenous population of tenocytes from iPSCs with high efficiency continues to be a challenge, largely in part to the limited understanding of their developmental origins and differentiation path from multipotential precursors.

In vertebrate embryogenesis, tendons arise from mesodermal cells of different origin. Axial, limb, and cranial tendons originate from paraxial mesoderm, lateral plate mesoderm or neural crest (NC), respectively. Despite differential cell and tissue interactions between the three regions, the major molecular regulators of tendon differentiation are shared between all three.[22,23] BMP, TGFβ, Activin/Nodal, FGF and WNT signaling pathways regulate mesoderm induction from pluripotent cells. Along the mediolateral axis of the embryo the balance between BMP and WNT signaling gradients specify mesodermal subtypes.[24,25] The paraxial or presomitic mesoderm (PSM) is derived from Neuromesodermal Progenitors (NMPs) that are bipotential and able to differentiate into ectodermal and mesodermal lineages.[24] Recent *in vitro* studies demonstrated that during mesoderm specification, WNT controls the allocation to PSM and represses lateral plate mesoderm.[25,26] Somites (SM) are derived from the anterior PSM following dynamic morphogenetic cyclic signaling, involving Notch, WNT and FGF.[24] Somite progenitors are multipotential and are further specified by signaling molecules from the surrounding tissues. Sonic hedgehog (SHH) is secreted from the notochord and the neural tube and it has been demonstrated as a crucial signaling modulator in sclerotome (SCL) specification of somites combined with low levels of WNT and BMP.[24,25] Murine and avian embryonic development studies concluded that combined SHH activation and BMP inhibition may be sufficient for SCL induction.[24] However, it was later shown *in vitro* that WNT directly antagonizes SHH and induces somites to dermomyotome.[25] Since SCL is in contact with different cell populations and thus diverging signals, it gives rise to different cell populations along the three major patterning

axes. SCL develops dorsally into the syndetome (SYN), the precursor of tendons of the body trunk, which is marked by the expression of the transcription factor scleraxis (SCX).[24] Recent studies have indicated that FGF, BMP and TGFβ are orchestrating syndetome differentiation from sclerotome.[15,16,27] A few groups have differentiated mouse iPSCs[15] and human iPSCs[27] to SYN through SCL and have pinpointed the primary role of BMP and TGFβ signaling. However, the nuances of WNT signaling in SYN specification have yet to be explored.

In this study, we sought to fine-tune induction to SYN by further elucidating the signaling pathways involved with tenocyte formation using single cell transcriptomics. SYN was induced from GMP-ready human iPSCs by stepwise differentiation through PSM-derived SM cells using chemically defined media. At every stage of the induction, we monitored known markers for each developmental step and conducted further characterization with single-cell RNA sequencing (scRNA-seq) and immunostaining. ScRNA-seq analysis revealed off-target differentiation towards a neural phenotype, with WNT family members being identified as crucial to the generation of neural by-products. We hypothesized that WNT signaling inhibition would block cell fate bifurcation to “unwanted” states and drive induction towards a single path. Informed by single cell transcriptomics, we added the WNT inhibitor Wnt-C59 to the later stages of the differentiation, which improved final induction efficiency of the differentiated tendon progenitor population.

Results

Stepwise induction of iPSCs to syndetome-like cells using chemically defined media and small molecules *in vitro*

Human iPSCs were seeded at different densities and induced to PSM for 4 days with the GSK3 inhibitor (GSK3i) CHIR99021 leading to WNT pathway activation, combined with BMP and TGFβ inhibition and concurrent FGF activation (**Fig. 1A**). Gene expression analysis, immunofluorescent staining (IF) and flow cytometry for DLL1 levels were used to determine induction efficiency and establish the starting seeding density (Suppl. Fig. 1). A homogeneous population of DLL1+ cells was generated after 4 days when cells were seeded at ~40-50 aggregates/cm[2]. Specifically, 96.2% DLL1$^+$ cells were generated at day 4 (Suppl. **Fig.1**). In contrast, DLL1$^+$ cells were shown to be 43.6% less (52.6% DLL1$^+$ cells) when iPSCs were seeded at 2x concentration.

Cells exhibited distinct morphologies at different stages of chemical induction (**Fig. 1B**). On day 4, iPSC colonies displayed contraction, resulting in differentiating cells leaving the colonies at the periphery. By day 8, cells were completely dissociated from the colonies. On day 11, colonies looked contracted and regressed, and were surrounded by spindly cells. Lastly, by the end of the differentiation period, fibroblast-like cells had grown in size. However, during SYN induction we noticed a gradual attrition of cells, resulting in considerably lower cell numbers at the end of the process.

To further characterize cell differentiation at each stage, the expression of PSM, SM and SCL stage cell markers was examined with RT-qPCR (**Fig. 1C-F**) and IF (**Fig. 2A-G**). Additionally, markers associated with tendon progenitors and tenocytes were examined as an indication of SYN differentiation (**Fig. 1G**, **Fig. 2H-I**). Pluripotency markers (OCT4, NANOG) were significantly downregulated at PSM compared to iPSC and were not detected at subsequent stages (**Fig. 1C**). PSM marker genes DLL1, TBX6, WNT3A and MSGN1[24,25] were significantly upregulated at day 3 and day 4 of GSK3i treatment and downregulated after 4 more days of TGFβ inhibition and WNT activation of DLL1$^+$ cells (**Fig. 1D**). Mesodermal T-box transcription factors TBX1 and TBX6[28] were detected at PSM stage (**Fig. 2C**) but not at SM stage (**Fig. 2C-D**). SM markers MEOX1, and PAX3[24,25] were upregulated at day 8, defining the somitogenesis stage (**Fig. 1E**, **Fig. 2C-E**). Following 3 days of BMP inhibition and SHH pathway activation of SM stage cells, SCL markers

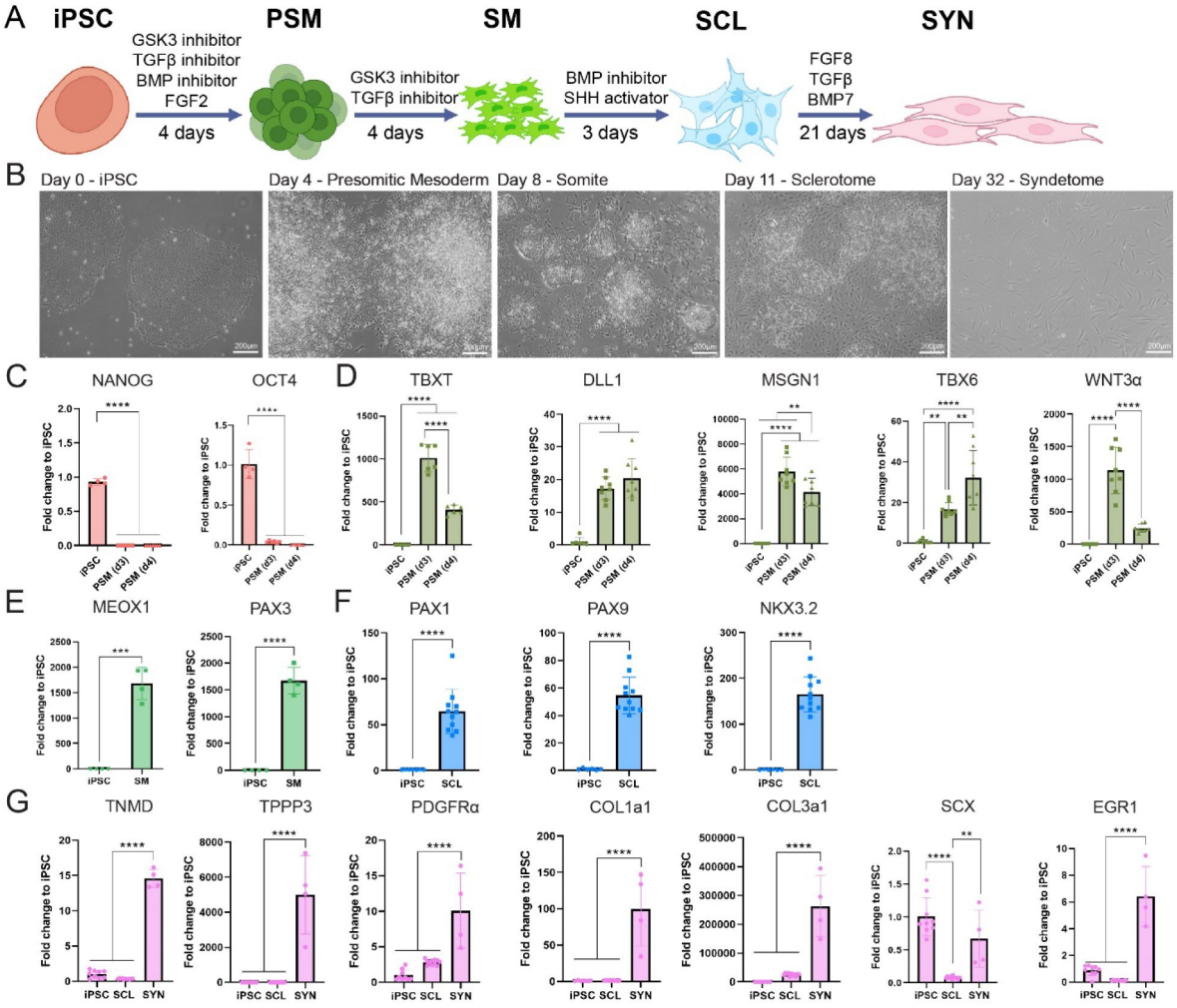

Fig. 1.

Stepwise induction of iPSCs to syndetome-like cells using chemically defined media and small molecules *in vitro.*

(A) Schematic of iPSC to SYN stepwise induction using chemically defined media and small molecules. **(B)** Brightfield micrographs of cells going through the differentiation stages at. Scale bars represent 200μm. **(C)** Pluripotent markers were expressed in iPSCs and were downregulated in further stages. **(D-F)** Gene expression analyses for stage-specific markers with the 007i iPSC line: upregulation of early mesoderm markers at the PSM (n=8 replicates/group) **(D)**, somitogenesis at SM (n=8 replicates/group) **(E)**, sclerotome-related markers at SCL (n=12) **(F)**. **(G)** Tenogenic markers are significantly upregulated at the SYN stage (n=4) compared to iPSC (n=9) and SCL (n=12) stages. Differentiation experiments were repeated independently n=2 with the 007i line and n=2 with a second iPSC line that was later tested (83i); *$p<0.05$, **$p<0.01$, ***$p<0.001$, ****$p<0.0001$.

(NKX3.2, PAX1 and PAX9)[24,25] were significantly upregulated at day 11 (**Fig. 1F**). PAX1 and PAX9 were observed in the entire cell population at SCL (**Fig. 2G**). PDGFRA and TPPP3[29] markers were significantly upregulated at the SYN stage (**Fig. 1G**). Interestingly, SCX, a prominent tenogenic transcription factor,[30] was significantly downregulated at the SCL stage compared to iPSC, but upregulated during the differentiation from SCL to SYN. Further, COL1A1, COL3A1 and TNMD[31] were significantly upregulated at the last stage of SYN induction (**Fig. 1G**). IF staining confirmed the presence of SCX^+COL1^+ and $TNMD^+COL1^+MKX^+$ cells at the end of the induction (**Fig. 2I**). However, expression of tenogenic markers was heterogeneous in different cells (**Fig. 2I**). Additionally, we noticed gradual attrition of cells after SCL stage, resulting in considerably lower cell numbers by the end of the differentiation.

Single-cell RNA sequencing reveals cellular heterogeneity at the end of induction of iPSC to syndetome-like cells

Even though gene expression and IF showed expression of early tendon markers by the end of differentiation using two iPSC lines (Suppl. Fig. 4A), cell heterogeneity was observed with IF (**Fig. 2**). Further, SYN differentiation efficiency was suboptimal, resulting in considerable cell attrition by the end of the induction process (**Fig. 1B**, **Fig. 2G-I**). To further explore the observed cellular heterogeneity, we sought to investigate the cell transcriptome at each stage (iPSC, PSM, SM, SCL, and SYN) at a single cell level using the GMP-ready line 007i and scRNA-seq analysis. The dimensional reduction based on the unsupervised UMAP method sorted cells into 11 clusters that could be classified as 6 cell subpopulations (**Fig. 3A**). Raw counts of cell numbers for each cluster and stage are shown in Suppl. Table 1 and normalized proportions per cluster in Suppl. Fig. 2. Feature plots and dot plots showed upregulation of stage-specific genes (**Fig. 3B-C**). That is, pluripotency markers (OCT4, NANOG, SOX2)[32] were expressed at iPSC and disappeared at the PSM stage, while PSM markers TBXT, TBX6, MSGN1, DLL1, DLL3[24,25,33] were upregulated. SM markers (MEOX1, PAX3)[24,25] and SCL markers (PAX1, PAX9, NKX3.2, SOX9)[24,25] were upregulated in a stepwise manner. Tenogenic markers (SCX, MKX, TNMD, COL1A1, DCN, COL3A1)[31,34] were found in SYN cluster C3 (**Fig. 3B-D**). These plots show that the SYN cluster accounted for 48.4% of the entire population (Suppl. Table 1 and Suppl. Fig. 2). Notably, two "side-arm" clusters, which became prominent in SCL, comprised of 18.3% of the cells collected at the SYN stage (**Fig. 3A**, Suppl. Table 1 and Suppl. Fig. 2). These were denoted as neuromesodermal progenitor – cranial cell populations hereafter referred to as NMP-C ($DLL1^+DLL3^+NOTCH1^+CRABP1^+$),[25,35,36] and neural lineage, hereafter referred to as NL ($NRN1^+DCX^+NNAT^+$),[37–39] cell populations.

Trajectory analysis shows off-target differentiation to neural-like progenitors

Monocle package (v2.22.0) was used to create pseudo-time trajectory (**Fig. 3E-F**) and branching point heatmaps (**Fig. 3G-H**). Examination of branch point heatmaps and marker expression showed that the "side-arm" clusters that predominated in the later SCL stage and especially in SYN (**Fig. 3A**), were enriched for neural-related markers NRN1, SYP, PCLO and DCX[38–40] (**Fig. 3I**). This suggests that these two clusters were likely side products that deviated from the main differentiation trajectory into neural lineage cell population.

To understand the pathways enriched at each induction stage, we used QIAGEN Ingenuity Pathway Analysis (**Fig. 3J-L**). Examining the canonical pathways in our dataset, we found that in SYN cluster, BMP activation was linked to differentiation towards the tenocyte lineage and concurrent WNT inhibition through DKK1 upregulation (**Fig. 3J**). Moreover, the side arm clusters showed activation of WNT signaling and upregulation of gene signatures associated with

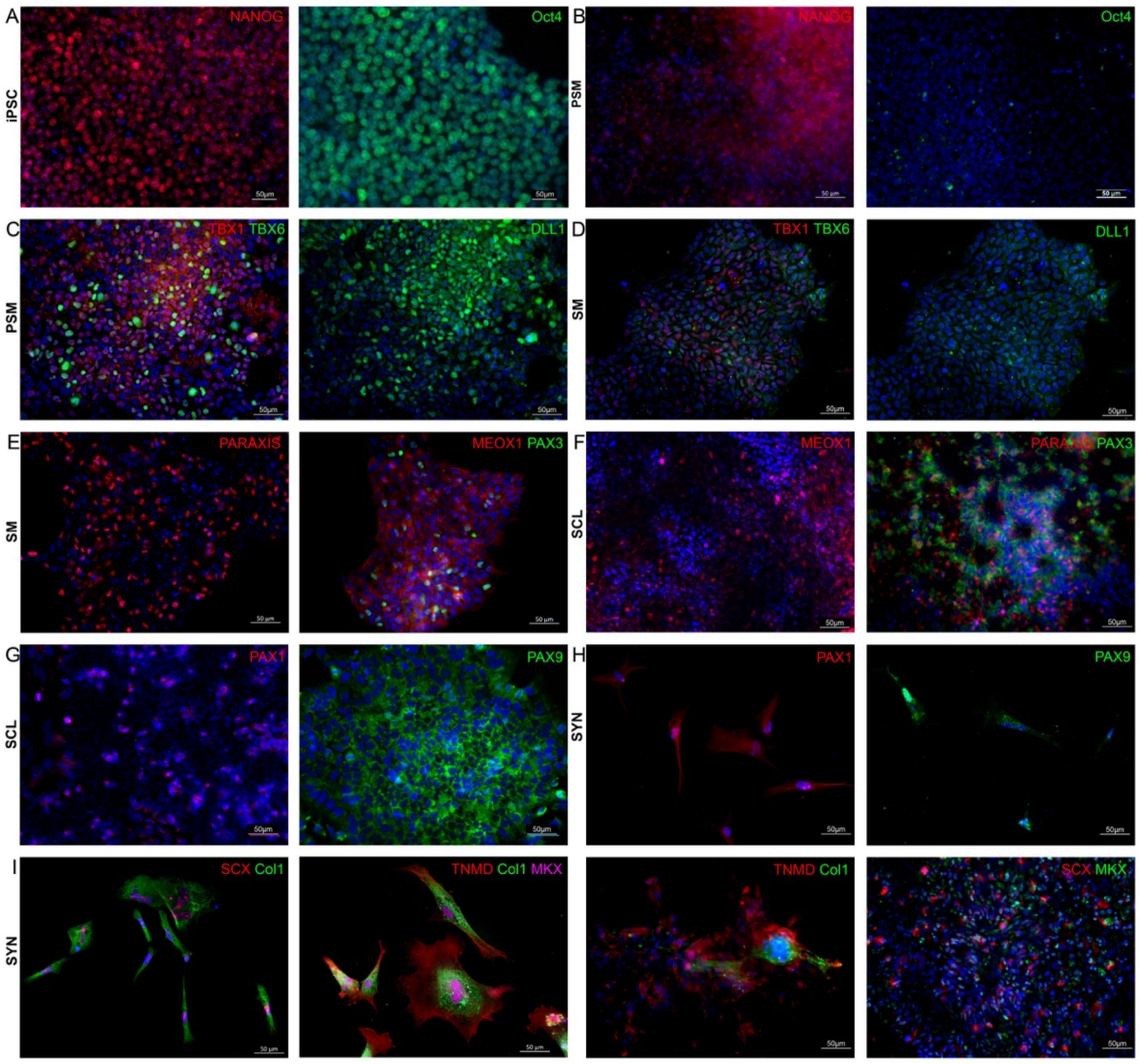

Fig. 2.

Immunofluorescence co-staining for stage-specific markers for confirmation of protein expression at each induction stage.

(A-B) OCT4 and NANOG were expressed in iPSCs but were downregulated at PSM. **(C-D)** Early mesoderm markers TBX1, TBX6 and DLL1 at PSM vs. SM. **(E-F)** Somitogenesis markers PARAXIS, MEOX1, and PAX3 at SM vs. SCL. **(G-H)** sclerotome-related markers PAX1 and PAX9 at SCL vs. SYN. **(I)** Tenogenic markers SCX, COL1, TNMD, MKX co-expression at the end of induction to SYN. Nuclei were stained with DAPI (blue). Scale bars represent 50μm. Differentiation experiments were repeated independently n=2 with the 007i line and n=2 with a second iPSC line that was later tested (83i). IF staining was performed in n=3 technical triplicates.

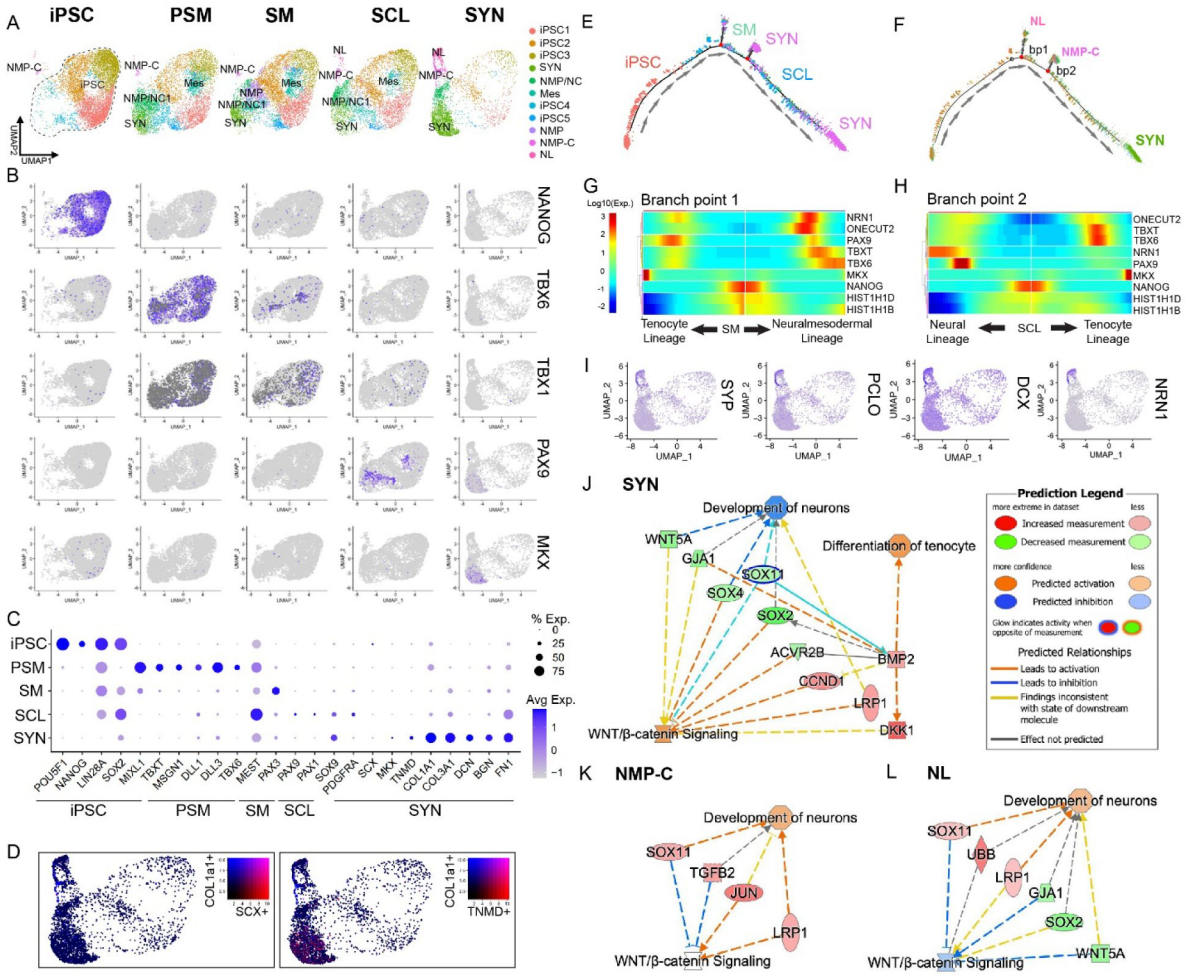

Fig. 3.

Single-cell RNA sequencing reveals cellular heterogeneity at the end of induction of iPSC to syndetome-like cells and off-target differentiation to neural-like progenitors.

(A) UMAPS of each differentiation step sorted into 11 cell clusters from iPSC to SYN were annotated to 6 distinct cell populations: iPSC (OCT4^{+}SOX2^{+}NANOG+), Syndetome (SYN, MKX^{+}TNMD^{+}COL1A1^{+}), Neuromesodermal Progenitors/Neural Crest cells (NMP/NC, PAX3^{+}NRP2^{+}COLEC12^{+}), Mesoderm (Mes, DLL1^{+}DLL3^{+}PARAXIS+), Neuromesodermal Progenitors – Cranial (NMP-C, DLL1^{+}DLL3^{+}NOTCH1^{+}CRAB1^{+}), and Neural Lineage cells (NL, NRN1^{+}DCX^{+}NNAT^{+}). During induction pluripotent clusters gradually disappeared, and three main clusters emerged: SYN, NMP-C, and NL. **(B-C)** Feature plots **(B)** and dot plots **(C)** of stage-specific genes displayed for all differentiation stages. **(D)** Expression of primary tenogenic markers COL1A1 (blue) and either SCX (red) or TNMD (red) on UMAP plot. **(E-F)** Original samples and clusters were ordered on pseudo-time developmental trajectory. **(E)** Trajectory analysis based on original samples showed transition from iPSC to SYN correlated with the samples, however, SYN cells were located within three endpoints. **(F)** Trajectory analysis based on clusters showed SYN cluster as the main differentiation endpoint with NMP-C and NL as off-target differentiation endpoints. Branching point heat maps **(G-H)** and gene expression were predominated by neural-related markers SYP, PCLO, DCX, and NRN1 **(I)**. **(J-K)** IPA analysis revealed that the off-target clusters NMP-C and NL clusters, were linked with increased Wnt pathway activity **(K-L)**, while SYN cluster was associated with tenocyte differentiation and linked to decreased Wnt pathway activity **(J)**.

neuronal development (**Fig. 3K-L**). In conclusion, iPSCs were successfully differentiated into SYN, however, cells expressing neural markers also appeared as side products during the differentiation, and WNT signaling was found to play a role in this process.

Inhibition of WNT signaling resulted in decrease in off-target differentiation

Pathway analysis showed that the crosstalk between BMP and WNT may play an important role in off-target differentiation products. Thus, we hypothesized that inhibition of WNT signaling may improve induction towards tenogenesis. We investigated the addition of a potent PORCN inhibitor, WNT-C59, which blocks both canonical and non-canonical WNT signaling (**Fig. 5A**). We observed that when WNT inhibitor (WNTi) was implemented after day 8 (SM stage), it resulted in decreased expression of neural markers NRN1, DYNLLl1 and FMN1 (**Fig. 4A**). Immunostaining for neural markers (DCX, SYP and NRN1) showed decreased expression in WNTi-treated cells (**Fig. 4C** 1-C3) unlike non-treated cells (**Fig. 4B** 1-B3). Implementation of the WNTi inhibitor also resulted in significantly higher expression of tenogenic marker TNMD partway through SYN induction (**Fig. 4A** 2). A higher proportion of $COL1^{+}TNMD^{+}$ and $SCX^{+}MKX^{+}$ cells were observed in SYN^{WNTi} compared to SYN group (**Fig. 4E-F**). Notably, in some cases we observed overgrowth of cells into spherical 3D structures (**Fig. 4D**), which could be related to the other cell populations comprising ~50% of this group (Suppl. Table 1 and Suppl. Fig. 2).

To further unveil the role of continuous WNT inhibition at the SM stage and until the end of the induction to SYN, we performed scRNA-seq (**Fig. 5A**). 5645 cells were subjected to unsupervised clustering and plotted with UMAPs. Integrated UMAP plots of all the cell populations in this study revealed 12 distinct clusters which were further characterized. We annotated 7 cell populations by using classical developmental markers and performing gene ontology enrichment analysis for DEGs (**Fig. 5B**). Six clusters expressed pluripotency and stem cell markers, including NANOG, OCT4, and SOX2 and were annotated as pluripotent cells (iPSC1-6). These populations were evident during the first stages of induction, and they gradually receded. At PSM stage two mesodermal populations were identified, one was annotated as Mes ($TBXT^{+}DLL1^{+}$) and another as NMP-C, where TWIST1,[25] SP5,[41] and SNAI2[42] were upregulated. These two populations further expanded at the SM stage. At the SCL stage, two additional newly formed clusters appeared. These were categorized as NL and neural crest (NC) cells. The NL cells expressed markers associated with neurogenesis including CRABP1, DCX, MAP2.[43] The NC cells expressed SOX4, SOX11, and NCAM1.[44,45] At the SYN stage we identified a SYN population with cells expressing tendon and ECM associated markers ($COL1A1^{+}$, $COL1A2^{+}$, $COL3A1^{+}$, $COL11A1^{+}$, $FN1^{+}$, $FBN1^{+}$, DCN^{+}). WNT inhibition resulted in the elimination of the NC population, while the SYN population has increased in size and a second population expressing tendon and some chondrogenic markers was evident, denoted as fibrocartilage (FC) cluster. The expression levels of classical stage-specific markers in SYN^{WNTi} presented in a dot plot showed increased expression compared to untreated SYN group (**Fig. 5C**). Density plots of cells expressing COL1A1 and tendon markers SCX and TNMD showed increased positive cells for those markers in SYN^{WNTi} compared to SYN group (**Fig. 5D**). Trajectory analysis for the WNTi-treated group showed elimination of the bifurcations that were observed in the non-treated group (**Fig. 5E**). Cell proportions for each cluster were calculated by normalizing to total cell numbers. It was shown that 75.6% of all cells in SYN^{WNTi} were clustered at the two SYN subpopulations, SYN and FC (66.9 and 8.7%, respectively; **Fig. 5F**). Comparison of WNTi treated groups using a second iPSC line (83i) showed that in the second line, 78% of cells were clustered in the SYN group, while the FC cluster was non-existent (Suppl. Fig. 3 and Suppl. Table 1).

IPA network analysis following treatment with the WNTi showed that WNT pathway activation is associated with the NMP-C and NC clusters and not with the SYN, NL, and FC clusters (**Fig. 5G**).

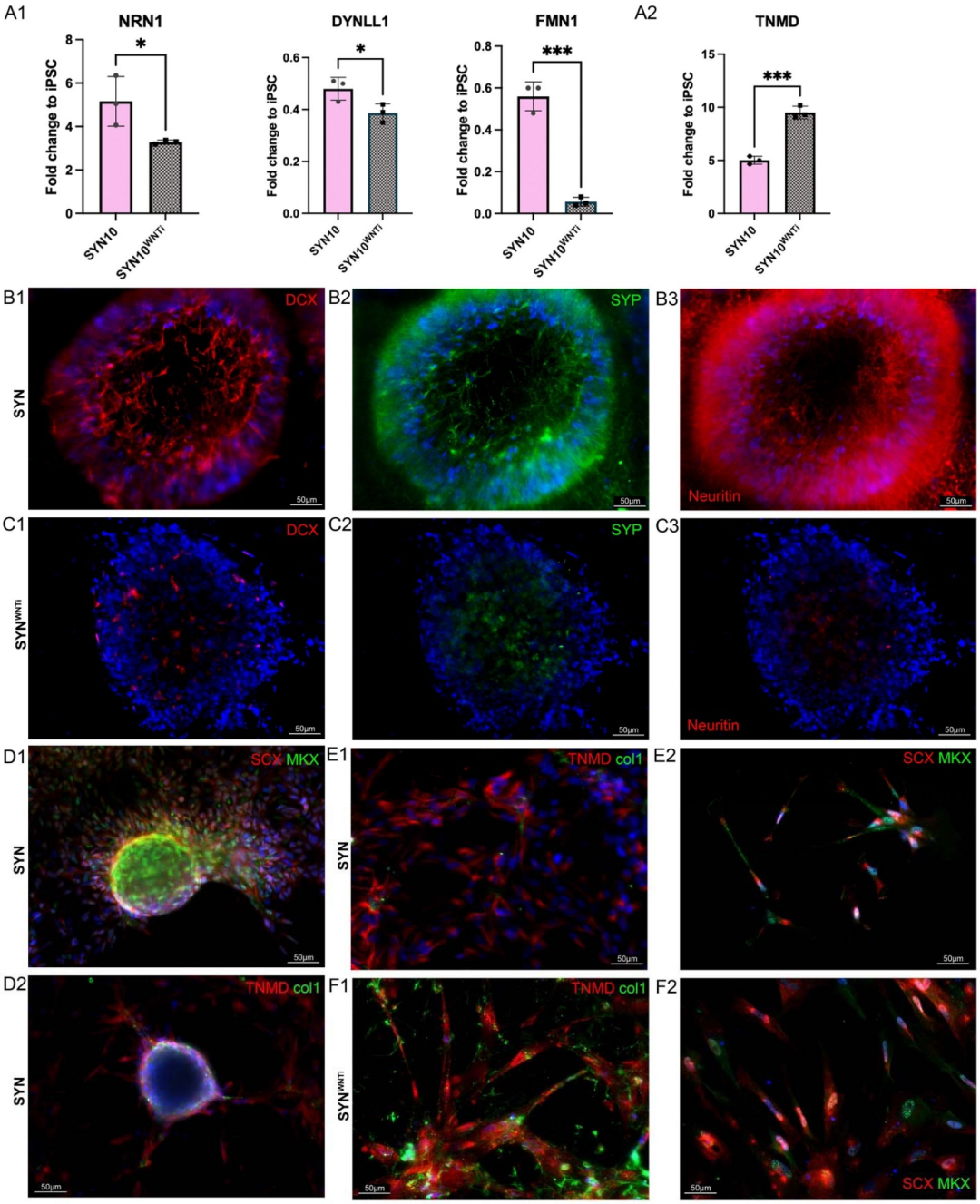

Fig. 4.

Inhibition of WNT signaling resulted in decreased expression of off-target markers and a more homogeneous population.

(A) Gene expression analysis of neural markers NRN1, DYNLL1 and FMN1, as well as tenogenic marker TNMD on day 10 of SYN induction (day 21 of the differentiation). **(A1)** Cells treated with WNTi had significantly downregulated neural marker expression compared to just SYN. n=4 replicates/group. **(A2)** Tendon gene expression was significantly upregulated in the WNTi-treated group; n=3/group; *p<0.05, **p<0.01, ***p<0.001, ****p<0.0001. **(B-C)** Immunofluorescence staining for neural markers (DCX, SYP, NRN1), SYN **(B1-B3)** and SYN^{WNTi} **(C1-C3)** showed that they were present in SYN and disappeared in SYN^{WNTi}. Scale bars represent 50µm. **(D-F)** Immunofluorescence staining for tenogenic markers (SCX, MKX, TNMD, COL1) of SYN and SYN^{WNTi} showed that more COL1^{+}TNMD^{+} and SCX^{+}MKX^{+} cells were observed in SYN^{WNTi} compared to SYN. Scale bars are 50µm. Differentiation experiments were repeated independently n=2 with the 007i line and n=2 with a second iPSC line that was later tested (83i). IF staining was performed in n=3 technical triplicates.

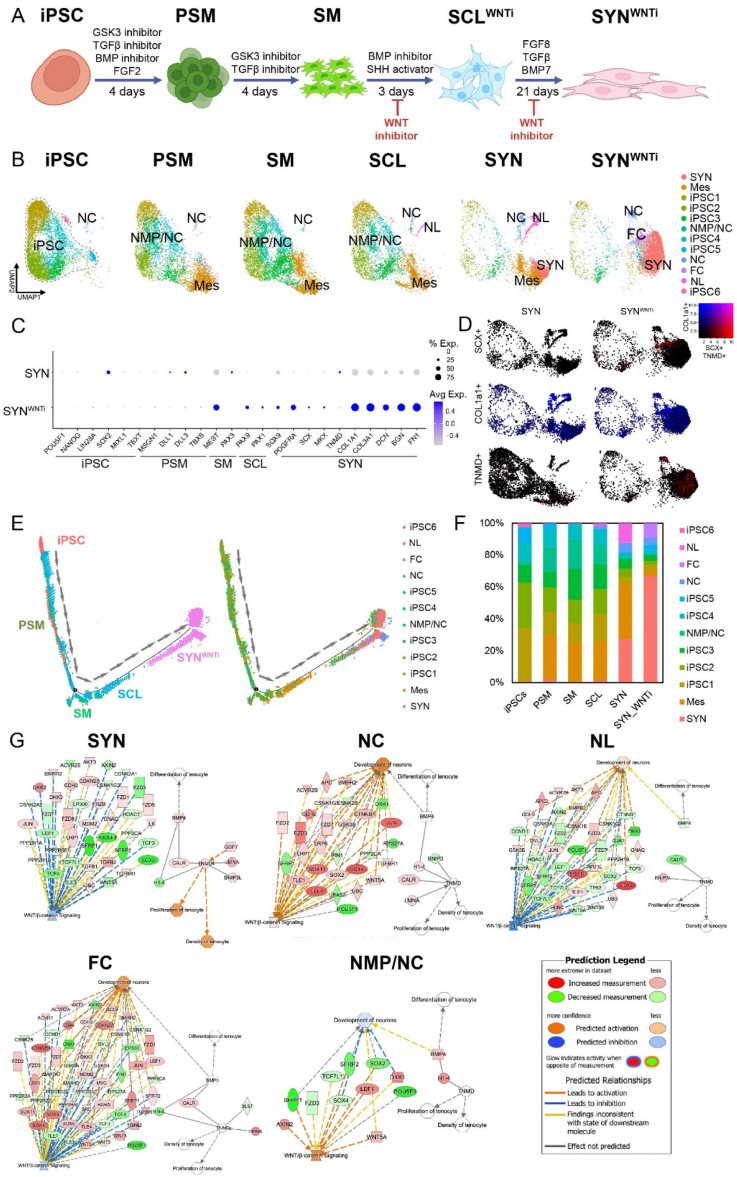

Fig. 5.

Addition of WNTi to the SCL and SYN induction stages of the differentiation improved differentiation to SYN and eliminated off-target clusters.

(A) Schematic of optimized iPSC to SYN stepwise induction with WNTi addition implemented at SM to SCL and SCL to SYN stages. Informed by single cell transcriptomics, the addition of Wnt pathway inhibitor at the later stages of the differentiation resulted in a more specific differentiation of iPSCs to tenocytes. **(B)** UMAPS of each differentiation step sorted into 12 distinct clusters from iPSC to SYN were annotated into 6 distinct cell populations: Syndetome (SYN, $MKX^{+}TNMD^{+}DCN^{+}BGN^{+}$), iPSC ($OCT4^{+}NANOG^{+}LIN28A^{+}SOX2^{+}$), Neuromesodermal Progenitors/Neural Crest (NMP/NC, $TBXT^{+}TWIST1^{+}SP5^{+}SNAI2^{+}$), Neural Crest (NC, $PTN^{+}NTKR2^{+}SOX4^{+}SOX11^{+}$), Fibrocartilage (FC, $COL2A1^{+}SOX9^{+}FN1^{+}BGN^{+}COL1a1^{+}$), Neural Lineage (NL, $SOX2^{+}DCX^{+}MAP2^{+}UNCX^{+}SOX4^{+}$). UMAP comparison of the SYN and SYN^{WNTi} populations demonstrated increased size of the SYN cluster and elimination of NL cluster. **(C)** Dot plots of gene expression of stage-specific genes for SYN and SYN^{WNTi}. **(D)** Expression of primary tenogenic markers Col1a1 (blue), Scx (red) and Tnmd (red) on UMAP plot for SYN and SYN^{WNTi}. **(E)** Original samples and clusters were ordered on pseudo-time developmental trajectory. Trajectory analysis revealed one main endpoint, the SYN cell populations. **(F)** After addition of WNTi, the proportion of cells in the SYN clusters increased by 59% while the proportion of cells in the NL cluster was eliminated. **(G)** IPA network analysis showed that WNT pathway was enriched in the NMP/NC and NC clusters but not in NL.

Discussion

In this study, informed by ontogenesis and recent reports modeling PSC differentiation *in vitro*, we successfully differentiated human iPSCs to syndetome-like cells in a stepwise manner using a GMP-ready line and chemically defined serum-free media through balancing the BMP, TGFβ Activin/Nodal, FGF, and WNT signaling pathways. iPSCs were differentiated to presomitic mesoderm, somite, sclerotome and syndetome-like cells (**Fig.1A**-B). Gene expression analysis, IF, and scRNA-seq analysis validated the stepwise differentiation using classical markers that define each developmental step. However, gene regulatory network analysis revealed that the major off-target cell populations were highly associated with WNT signaling activation beginning from the SCL stage and into the SYN stage. Using scRNA-seq, we confirmed our hypothesis that WNT inhibition with the WNT signaling inhibitor (WNTi) Wnt-C59 blocked cell fate bifurcation to the "unwanted" neural fates and drove induction towards tenogenesis.

Gene expression analysis showed significant upregulation of stage-specific markers (**Fig. 1C-G**). PSM induction was assessed via the Notch receptor ligand Delta-like protein-1 (DLL1) gene and protein expression. Somites form from the epithelization and segmentation of paraxial mesoderm along the rostro-caudal (RC) axis of the embryo in the process of Mesenchymal to Epithelial Transition (MET). Studies in several animal models have shown that that somite RC polarity is established prior to SM formation and it is orchestrated by NOTCH signaling.[24] Many DLL-family proteins, which are NOTCH receptor ligands, are central to this process, with DLL1 shown as the most critical during PSM formation.[35,46] Here, we found that the initial seeding density of iPSCs impacted DLL1 expression and thus induction efficiency. Higher starting densities resulted in decreased $DLL1^+$ cell ratios assessed by flow cytometry (Suppl. Fig. 1). This is in line with several reports that have identified starting PSC seeding density as an additional factor influencing cell differentiation in animal models and human cells.[47] This could be attributed to auto/paracrine factors and cell-cell contact.[48] Unfortunately, iPSC seeding density is often not reported in published protocols and it may be contributing to discrepancies and reproducibility concerns between different laboratories. Taken together, our data indicate that starting seeding density is a crucial component of chemical induction which could influence reproducibility and translatability of a given approach.

Somitogenesis induction was achieved by TGFβ inhibition (SB431542) and moderate WNT activation (CHIR99021) similar to previous reports.[26] Combined SHH signaling activation (SAG) and BMP inhibition (LDN193189) resulted in induction of SM to SCL. Last, stepwise FGF8 followed by BMP and TGFβ administration induced SYN formation. Early tendon-associated markers were significantly upregulated at the final timepoint of SYN induction (**Fig. 1G**). FGF ligands including FGF8 are secreted by the myotome region of the somite, located next to the sclerotome, inducing Scleraxis (SCX) expression, which in turn drives syndetome specification.[24] Protein expression at each stage was verified with IF (**Fig. 2**). However, at the end of differentiation we noticed gradual cell attrition in the cultures (**Fig. 1B**, 2I). This could be attributed to the heterogeneity of the cell population at SCL stage, which was confirmed by scRNA-seq (**Fig. 3A**).

In the current study, scRNA-seq analysis showed that mesodermal cells persisted until SYN induction (**Fig. 3A-C**). DLL1 expression was significantly upregulated at PSM and downregulated at SM stage. At PSM, 96.2% of the cell population was $DLL1^+$ (Suppl. Fig. 1). However, dot plots showed some DLL1 and DLL3 expression in all stages and clusters (**Fig. 3C** and Suppl. Fig. 4). Consequently, using a single marker may not be sufficient to assess lineage differentiation efficiency. Trajectory analysis showed two distinctive bifurcations at SM and SCL stages. The first branchpoint was observed at the SM stage, when a Mes ($DLL1^+DLL3^+PARAXIS^+$) and a transient NMP ($PAX3^+NRP2^+COLEC12^+$) cell population were identified. NMPs were present at SM and disappeared thereafter, while at SCL two "side-arm" clusters evolved (**Fig. 3A**). The

NL cluster was enriched for several neural-associated markers ($NRN1^+NNAT^+CRABP1^+ONECUT2^+NPTX2^+$). In the NMP-C side-arm cluster the top DEGs were a combination of neural-associated markers ($NOTCH1^+CRABP1^+GREB1^+ID4^+$), cranial mesodermal markers ($DLL1^+DLL3^+$) and ECM genes including collagens and FN1. The emergence of these two off-target cell populations became quite prominent at SCL, while they were further amplified at SYN (**Fig. 3A**).

Sclerotome is derived from the ventromedial part of somites and its induction is orchestrated by SHH.[24] It is established that SHH and NOG produced in the notochord and neural tube stimulate MET, which produces both NC cells from the ectoderm as well as SCL at the ventromedial aspect of somites.[49] Different groups have achieved sclerotome induction of iPSCs with varying approaches. For instance, Loh *et al* identified that WNT and SHH acted antagonistically in SCL specification.[25] The NMP-C off-target cell population that was first observed in the SCL and SYN groups could have arisen from NMPs (**Fig. 3A**). NC, which are a transient cell population of ectodermal origin, are derived from bipotential NMPs from the primitive streak in the presence of FGF, WNT and likely medium BMP activity.[50,51] However, the timing and levels of BMP signaling required for NC differentiation are still not well understood. Wu *et al*[12] observed NC off-target populations during stepwise iPSC to somite to chondroprogenitor differentiation. In that study, the authors first observed NC at the chondroprogenitor stage, and hypothesized that they emerged due to BMP treatment for 3 days at the SCL stage.[12] In the present study, we observed the emergence of NC cells earlier and even though we applied a BMP inhibitor during the SM to SCL differentiation, it may not have been sufficient to modulate BMP activation. Lastly, the NC off-target population could have been derived from NMP/NC cells or from NMPs present at SM. *In vivo* somites give rise to the dermatome and myotome dorsally and the SCL ventromedially.[24] The dermatome sits next to the ectoderm and can differentiate into the meningotome which can form spinal meninges as well as fibroblasts of the meninges and arachnoids.[52] The off-target neural cluster in the present study showed increased expression of markers associated with NC as well as neural markers. Thus, it could be posited that it was derived from the NC off-target subpopulation identified at SCL.

Next, DEG analysis using the IPA platform revealed the interaction between WNT and BMP signaling at the cornerstone between the SYN cluster and the NL and NC off-target “side-arm” clusters (**Fig. 3J-L**). More specifically, upregulation of genes associated with WNT signaling activation in both off-target clusters were observed. Therefore, a WNT pathway inhibitor was employed during SCL and SYN differentiation, which resulted in significant downregulation of selected neural markers, assessed by RT-qPCR and IF (**Fig. 4**).

Treatment with the WNTi following the SM stage resulted in the expansion of the SYN clusters (**Fig. 5A**) as well as complete elimination of the NL off-target cluster (**Fig. 5A**). Further, a new cell population was observed only in the WNTi-treated group, expressing some chondrogenic markers ($COL2A1^+SOX9^+FN1^+BGN^+COL1A1^+$), tenogenic genes and Klf transcription factors, which were recently shown to be associated with bipotential tendon-to-bone attachment cells.[53] In the same study, these cells were shown to activate a combination of tendon and chondrogenic transcriptomes. Fibrocartilage is found in the enthesis of tendons and shares the same progenitors as the syndetome.[54,55] Intriguingly, the FC cluster was not observed in the second cell line we differentiated (Suppl. Fig. 3) and it was the only observed difference between the two lines. Fibrocartilage progenitors express SCX, however, divergence of SCX^+ cells towards tendon or fibrocartilage have yet to be fully understood. In this work, WNT inhibition at the SM stage resulted in increased numbers of SCX^+ derivatives compared to SYN while eliminating the NL population. However, the NC cell population was not diminished, indicating that these cells might have been generated due to “contaminating” multipotential NMPs still present at SM and SCL. IPA network analysis revealed WNT pathway activation in mesodermal and NC clusters and not the final products of the induction, that is NL, FC, and SYN clusters (**Fig. 5G**). This further confirms our hypothesis regarding its activation following SM specification and suggests that it plays an

important role in specifying the fate of NMPs towards neural lineages. Further studies are needed to delineate the level of BMP activity required to either induce or block bifurcation of NMPs to NC fates. Interestingly, SCX expression peaked in the middle of SYN induction and decreased at the end (Suppl. Fig. 5), when TNMD, COLA1A and other tenogenic markers (collagens, DCN, BGN1, FN1) were upregulated. This suggests that SYN induction could be further optimized and shortened. Further, WNT inhibition during the entirety of the SYN induction might potentially negatively impact SYN maturation and it should be further fine-tuned. For instance, WNT signaling has been shown to upregulate TNMD expression in equine BM-MSCs,[56] while it was shown to suppress TNMD and other tenogenic genes in tendon-derived cells *in vitro*.[57]

Previous studies investigating iPSC to SYN differentiation reported varying yields at the end of induction. Nakajima *et al* reported 68% SCX+ cells using flow cytometry.[26] In a follow up study, the same research group reported 91.6% SCX+, 90.4% MKX+, 79.9% COL1A1+ and 77.5% COL1A2+ protein expression using IF quantification.[14] However, although informative, it could be noted that IF is only a semi-quantitative assessment burdened with operator bias and lower sensitivity compared to flow cytometry or scRNA-seq, unless performed in a more automated manner.[58] Nevertheless, despite those caveats, the high individual expression of all four markers (77.5%-91.6%) with IF supports a relatively efficient SYN differentiation overall. Kaji *et al* differentiated mESCs from SCX-GFP reporter mice to SYN and reported 90% efficiency assessed by flow cytometry for SCX,[15] while Sugimoto *et al* showed 66% efficiency utilizing a similar Scx-GFP mouse model combined with flow cytometry and scRNA-seq assessments.[15,16] In the current study, SYN clusters, characterized by scRNA-seq analyses, greatly increased in the SYN^{WNTi} group, from 47.6% prior to WNTi application, to 67%-78% of total cells after treatment (**Fig. 5F** and Suppl. Fig. 3). In conclusion, we showed that WNT inhibition was able to successfully modulate the later stages of differentiation from SM to SYN.

This study is not without limitations. The IPA network analysis is a knowledge-based and hypothesis driven platform. We have specifically targeted known pathways to be involved in syndetome differentiation. However, WNT signaling stood out with very specific affinity to the off-target populations and we have verified our findings with experiments proving this hypothesis. The SCL to SYN induction, maturation, and expansion in culture was considerably long and resulted in decreased expression of SCX (Suppl. Fig. 5), suggesting that it could be shortened. Even though following WNTi treatment induction efficiency increased considerably, there were still other populations present, including NC and undifferentiated cells. Cell sorting could be used to isolate a more homogeneous cell population. Further, removal of undifferentiated cells is crucial for *in vivo* preclinical studies. Future work is warranted to assess the functionality of the cells *in vivo*.

Conclusions

Tendons have poor innate healing capacity and novel approaches are urgently needed. Tendon cell therapy offers potential for regeneration of injured tissues. In this study, we successfully differentiated a GMP-ready human iPSC line to syndetome-like cells in a stepwise manner using fully defined media. However, scRNA-seq trajectory analysis revealed off-target differentiation towards a neural phenotype, resulting in heterogeneous differentiation. Differentially expressed gene and regulatory network analyses demonstrated WNT-associated effectors implicated in the off-target groups, which prompted us to apply a WNT inhibitor at the somite stage. Taken together, our data provide evidence that by manipulating WNT signaling we can achieve a more specific and robust differentiation of iPSCs to tendon progenitors. Elucidating the mechanism of the WNT signaling pathway using a development-inspired protocol can lead to the development of more powerful and specific differentiation protocols for cell therapy applications. iPSC-derived tendon progenitors can be an off-the-shelf cell source to tendon and ligament injuries that are currently untreatable or have poor surgical outcomes.

Acknowledgements

This study was supported by Cedars-Sinai Board of Governors Regenerative Medicine Institute, the NIH/NIAMS K01AR071512 (DS), California Institute for Regenerative Medicine DISC0-14350 and EDUC4-12751 (WJ) awards.

Additional information

Author contributions

Conceptualization, AP and DS; Methodology, AP and DS; Software, WJ and JS; Validation, AP, VY, WJ and JS; Formal analysis, AP, VY and WJ; Investigation, AP, VY, TS, AC, CC and MC; Resources, AP, VY and JS; Data Curation, WJ and JS; Writing-Original Draft, AP, VY and DS; Visualization, VY, AP and JS; Funding Acquisition, DS and WJ.

Declaration of interests

The authors declare no competing interests.

STAR Methods

Resource availability

Lead contact

Further information and requests for resources, reagents, data, and code should be directed to the corresponding author, Dmitriy Sheyn (Dmitriy.Sheyn@csmc.edu).

Materials availability

This study did not produce any unique reagents or materials.

Data and code availability

The raw sequencing data and original data are accessible in Gene Expression Omnibus. The series accession number is GSE229008. The original code is accessible at GitHub: *https://github.com/jason199112345/scRNA-seq-for-the-project-of-iPSC-to-Tenocyte-differentiation.git*.

Experimental model and subject details

iPSC maintenance and expansion

Human iPSC lines were obtained from the Cedars-Sinai Core facility and were expanded on Matrigel^{TM}-coated plates (BD Biosciences) (0.08 mg/well in 6 well plates). Cells were fed every other day with cGMP mTeSR™Plus media (StemCell Technologies) and passaged with ReLeSR™ (StemCell Technologies). Two distinct fully characterized hiPSC lines were used in this study: the GMP-ready CS0007iCTR-n5 line and the CS83iCTR-22n1 line (https://biomanufacturing.cedars-sinai.org/?filter_cell-type=ipsc&filter_primary-tissue&filter_disease&filter_sex&filter_age-at-sampling&filter_ethnicity&filter_race&filter_gene&filter_mutation&filter_project&cs_product_search).

Method details

iPSC to SYN differentiation

iPSCs were seeded into Matrigel-coated plates (#354230, Corning, Corning, NY) (0.08 mg/well in 6 well plates and 0.04mg/well in 12 well plates) and were induced to presomitic mesoderm (PSM) at 30% confluency (~50-60 aggregates/cm^2) in basal medium (BM) composed of IMDM/Ham's F12 (1:1) (Thermo Fisher), 1% lipid concentrate (Thermo Fisher), 0.5% antibiotic-antimycotic solution (Thermo Fisher), 15 µg/mL apo-transferrin (Sigma), 450µM monothioglycerol (Sigma), 7µg/mL insulin (Sigma) supplemented with 10 µM SB431542 (Sigma), 2µM DMH1 (Santa Cruz Biotechnology), 20ng/mL FGF2 (Biogems-PeproTech), and 10µM CHIR99021 (Biogems-PeproTech) (PSM media). After 3 days, media were changed to fresh PSM media. Geltrex (#A1413301, Thermo Fisher) was diluted 1:100 in cold serum-free DMEM/F12 to coat wells in 12-well plates (0.5mL/well). The coated plates were incubated for at least 1hr at 37°C before use. At day 4, PSM cells were washed with PBS and lifted using Accutase (StemCell Technologies) for 5min at 37°C and reseeded at 28,500 cells/cm^2 into the Geltrex-coated plates supplemented with SM differentiation media composed of BM supplemented with 10µM SB431542, 5µM CHIR99021, and 10µM Y-27632 dihydrochloride (Biogems, CA, USA). On days 5 and 7, media were changed to fresh SM media without Y-27632 dihydrochloride. At day 8, cells were cultured in sclerotome (SCL) differentiation media containing BM supplemented with 100nM SAG (Biogems-PeproTech), and 0.6µM LDN193189 (Biogems-PeproTech). Media were changed to fresh SCL media at day 10. At day 11, cells were washed with PBS, lifted using Accutase (StemCell Technologies) for 5min at 37°C and were reseeded at 60,000 cells/cm^2 into Geltrex-coated (Thermo Fisher) plates with BM supplemented with 20ng/mL FGF8 (Peprotech). After 3 days, media were changed to BM supplemented with 10ng/mL TGFβ3 (StemCell Technologies), and 10ng/mL BMP7 (PeproTech) (SYN maturation, SYN-M media). Media were changed to fresh SYN-M media every 3 or 4 days until day 32.

Application of Wnt inhibitor

Following initial single cell analyses, the iPSC to SYN induction was repeated with the addition of the Wnt signaling inhibitor Wnt-C59 (Cayman Chemical, MI, USA) beginning from the SCL induction stage and onwards; the somite cells treated with SCL media and sclerotome cells treated with SYN-M media were supplemented with 1µM Wnt-C59.

Flow cytometry

For assessment of DLL-1 levels to determine induction efficiency, cells that were induced for 4 days were lifted using Accutase for 5min at 37°C and washed 3x with FACS buffer containing 2% bovine serum albumin (BSA, A4503, Sigma, St. Louis, MO) and 0.1% sodium azide (S2002, Sigma) in PBS. The cells were either unstained, labeled with DLL1 anti-human antibody (APC-Vio 770, #130-106-148, Miltenyi Biotec, Bergisch Gladbach), or labeled with its associated isotype control (APC-Vio 770, #130-113-759, Miltenyi Biotec) for 15min protected from light at 4°C. After the incubation, cells were washed again and resuspended with FACS buffer. Data was acquired on a BD LSR Fortessa analyzer (BD Biosciences, San Jose, CA) and was analyzed using FlowJo software (FlowJo LLC, Ashland, OR).

Gene expression analysis

Differentiation to SYN was defined based on expression of developmental stage-specific markers (Supplemental Table 1). Cells were collected from each developmental stage and total RNA was isolated using the RNeasy plus kit (Qiagen), and reverse transcribed with the high-capacity cDNA reverse transcription kit (Applied Biosystems). Then, cDNA was amplified by performing qPCR with TaqMan® gene expression. The threshold cycle (Ct) value of 18S rRNA was used as an internal

control using the TaqMan® gene expression FAM/MGB probe system (4333760F, Thermofisher). The Livak method was used to calculate ΔΔCt values and fold change was calculated as $2^{-\Delta\Delta Ct}$, as previously described and published.[59]

Immunocytochemistry for phenotype confirmation

In preparation for immunocytochemistry, iPSCs were seeded onto coverslips. The coverslips were coated with Cultrex Poly-D-Lysine (R&D Systems) for 5min at RT, aspirated, and air-dried for at least 2h. They were then coated with Matrigel as per the seeding protocol described previously. At each developmental stage, cells were fixed with 4% paraformaldehyde for 30min at RT, followed by 3x PBS washes. Briefly, after serum-free protein blocking (X0909, Dako, Agilent), cells were hybridized with various primary antibodies (Table 1) overnight at 4°C. The following day, these cells were incubated with fluorophore-conjugated secondary antibodies (1h at 37°C). Coverslips were mounted onto slides using ProLong® Gold with DAPI (Molecular Probes, Life Technologies). A Carl Zeiss fluorescence microscope (Imager, Z1, ApoTome and MBF equipped) was used to acquire images.

Single cell RNA sequencing sample preparation, sequencing, and data processing

At each developmental stage (iPSC, PSM, SM, SCL, SYN, SYN^{WNTi}), cells were washed with PBS and lifted using Accutase (StemCell Technologies) for 5min at 37°C, and then centrifuged for 3min at 1000RPM. The cells were then resuspended in media, filtered using a 40 μM FlowmiTM cell strainer (Thermo Fisher) and washed twice more with media before being filtered for the last time to ensure a single cell suspension. The filtered cells were manually counted in quadruplicate with 0.4% trypan blue dye (Thermo Fisher) and cells were resuspended in media at a concentration of 1,500 cells/μL.

Single-cell RNA-Seq libraries were prepared per the Single Cell 3' v3.1 Reagent Kits User Guide (10x Genomics, Pleasanton, California) using the 10x Genomics Chromium Controller. Barcoded sequencing libraries were quantified by quantitative PCR using the Collibri Library Quantification Kit (Thermo Fisher Scientific, Waltham, MA). Libraries were sequenced on a NovaSeq 6000 (Illumina, San Diego, CA) as per the Single Cell 3' v3.1 Reagent Kits User Guide, with a sequencing depth of ~40,000 reads/cell.

Raw sequencing data was demultiplexed and converted to FASTQ format by using bcl2fastq v2.20 (Illumina, San Diego, California). More than 200 million reads were obtained for each sample. Reads were mapped to the human GRCh38 genome and count quantification was done using 10x Genomics Cell Ranger v.7.0.0.

We utilized our previously established single-cell analysis platform based on R (v4.1.2) [60]. Seurat package (v4.1.0) was used to load and process the single-cell data. Specifically, the data for each sample were loaded using *Read10X*. Quality control was performed for each sample. The parameters used for quality control were *nFeature_RNA*, that is the counts of genes detected in each cell, and *percent.mt*, that is the percent of mitochondrial genes expressed in each cell. Any cells having *nFeature_RNA* outside of the range of 200-8000 were excluded in the downstream analysis. Any cells with the *percent.mt* being smaller than 20%, were excluded in the downstream analysis. The Seurat object for each sample after the quality control was combined into a larger Seurat object. The large Seurat object was then normalized, anchored, and integrated. Principal component analysis with PC=30 was performed, dimensional reduction with Uniform Mani-fold Approximation and Projection (UMAP) was applied, and clusters were identified in an unsupervised manner with a resolution of 0.5. Following the identification of clusters, each cell was annotated with two important identities: the sample they were derived from, and the cluster (cell type) they belonged to. The differentially expressed genes (DEG) were calculated by comparing across sample identity or cluster identity, i.e., a specific cluster vs. all cells, a specific

sample vs. all other samples, a specific sample vs. another specific sample, or as otherwise noted in the manuscript. The DEGs were inputted to Qiagen Ingenuity Pathway Analysis (IPA) for gene ontology (GO) term enrichment and pathway analysis. Genes with $p<0.0001$ were included in the Qiagen IPA analysis.

The pseudo-time trajectory was constructed using the Monocle package (v2.18.0). The previously combined large Seurat object was loaded into the Monocle package. DDRTree method was used to reduce the dimension of the data. The cells were projected on the trajectory and visualized based on their identity or marker expression.

Statistical analyses

Data are presented as mean ± standard deviation from the mean. Normally distributed data were analyzed with unpaired t-test (for 2 groups), or non-repeated measures analysis of variance followed by Tukey-Kramer HSD *post hoc* analysis when more than 2 groups were compared. Non-parametric data were analyzed using the Mann-Whitney and Kruskal-Wallis tests. Statistical significance was set at $p<0.05$.

References

1. Yang G., Rothrauff B.B., Tuan R.S. (2013) **Tendon and ligament regeneration and repair: clinical relevance and developmental paradigm** *Birth Defects Res C Embryo Today* **99**:203–222 https://doi.org/10.1002/bdrc.21041

2. Liu W., Yin L., Yan X., Cui J., Liu W., Rao Y., Sun M., Wei Q., Chen F. (2017) **Directing the Differentiation of Parthenogenetic Stem Cells into Tenocytes for Tissue-Engineered Tendon Regeneration** *Stem Cells Transl Med* **6**:196–208 https://doi.org/10.5966/sctm.2015-0334

3. Webster K.E., Feller J.A., Leigh W.B., Richmond A.K. (2014) **Younger patients are at increased risk for graft rupture and contralateral injury after anterior cruciate ligament reconstruction** *Am J Sports Med* **42**:641–647 https://doi.org/10.1177/0363546513517540

4. Puetzer J.L., Ma T., Sallent I., Gelmi A., Stevens M.M. (2021) **Driving hierarchical collagen fiber formation for functional tendon, ligament, and meniscus replacement** *Biomaterials* **269**

5. Cai J., Xie X., Li D., Wang L., Jiang J., Mo X., Zhao J. (2020) **A novel knitted scaffold made of microfiber/nanofiber core–sheath yarns for tendon tissue engineering** *Biomaterials Science* **8**:4413–4425

6. Ho J.O., Sawadkar P., Mudera V. (2014) **A review on the use of cell therapy in the treatment of tendon disease and injuries** *Journal of Tissue Engineering* **5**

7. Abbah S.A., Spanoudes K., O'Brien T., Pandit A., Zeugolis D.I. (2014) **Assessment of stem cell carriers for tendon tissue engineering in pre-clinical models** *Stem cell research & therapy* **5**:1–9

8. Jo C.H., Lim H.J., Yoon K.S. (2019) **Characterization of Tendon-Specific Markers in Various Human Tissues, Tenocytes and Mesenchymal Stem Cells** . *Tissue Eng Regen Med* **16**:151–159 https://doi.org/10.1007/s13770-019-00182-2

9. Wang S. *et al.* (2013) **Human iPSC-Derived Oligodendrocyte Progenitor Cells Can Myelinate and Rescue a Mouse Model of Congenital Hypomyelination** *Cell Stem Cell* **12**:252–264 https://doi.org/10.1016/j.stem.2012.12.002

10. Kanke K., Masaki H., Saito T., Komiyama Y., Hojo H., Nakauchi H., Lichtler Alexander C., Takato T., Chung U.-i., Ohba S. (2014) **Stepwise Differentiation of Pluripotent Stem Cells into Osteoblasts Using Four Small Molecules under Serum-free and Feeder-free Conditions** *Stem Cell Reports* **2**:751–760 https://doi.org/10.1016/j.stemcr.2014.04.016

11. Yamashita A., Morioka M., Yahara Y., Okada M., Kobayashi T., Kuriyama S., Matsuda S., Tsumaki N. (2015) **Generation of Scaffoldless Hyaline Cartilaginous Tissue from Human iPSCs** *Stem Cell Reports* **4**:404–418 https://doi.org/10.1016/j.stemcr.2015.01.016

12. Wu C.-L., Dicks A., Steward N., Tang R., Katz D.B., Choi Y.-R., Guilak F. (2021) **Single cell transcriptomic analysis of human pluripotent stem cell chondrogenesis** *Nature communications* **12**

13. Komura S., Satake T., Goto A., Aoki H., Shibata H., Ito K., Hirakawa A., Yamada Y., Akiyama H. (2020) **Induced pluripotent stem cell-derived tenocyte-like cells promote the regeneration of injured tendons in mice** *Scientific reports* **10**

14. Nakajima T., Ikeya M. (2021) **Development of pluripotent stem cell-based human tenocytes. Development** *Growth & Differentiation* **63**:38–46

15. Kaji D.A., Montero A.M., Patel R., Huang A.H. (2021) **Transcriptional profiling of mESC-derived tendon and fibrocartilage cell fate switch** *Nature Communications* **12**

16. Yoshimoto Y., Uezumi A., Ikemoto-Uezumi M., Tanaka K., Yu X., Kurosawa T., Yambe S., Maehara K., Ohkawa Y., Sotomaru Y. (2022) **Tenogenic Induction From Induced Pluripotent Stem Cells Unveils the Trajectory Towards Tenocyte Differentiation** *Frontiers in Cell and Developmental Biology* **10**

17. Donderwinkel I., Tuan R.S., Cameron N.R., Frith J.E. (2022) **Tendon tissue engineering: Current progress towards an optimized tenogenic differentiation protocol for human stem cells** *Acta Biomaterialia*

18. Brown J.P., Galassi T.V., Stoppato M., Schiele N.R., Kuo C.K. (2015) **Comparative analysis of mesenchymal stem cell and embryonic tendon progenitor cell response to embryonic tendon biochemical and mechanical factors** *Stem cell research & therapy* **6**:1–8

19. Havis E., Bonnin M.-A., Olivera-Martinez I., Nazaret N., Ruggiu M., Weibel J., Durand C., Guerquin M.-J., Bonod-Bidaud C., Ruggiero F. (2014) **Transcriptomic analysis of mouse limb tendon cells during development** *Development* **141**:3683–3696

20. Havis E., Bonnin M.-A., Esteves de Lima J., Charvet B., Milet C., Duprez D. (2016) **TGFβ and FGF promote tendon progenitor fate and act downstream of muscle contraction to regulate tendon differentiation during chick limb development** *Development* **143**:3839–3851

21. Dale T.P., Mazher S., Webb W.R., Zhou J., Maffulli N., Chen G.-Q., El Haj A.J., Forsyth N.R. (2018) **Tenogenic differentiation of human embryonic stem cells** *Tissue Engineering Part A* **24**:361–368

22. Schweitzer R., Zelzer E., Volk T. (2010) **Connecting muscles to tendons: tendons and musculoskeletal development in flies and vertebrates** *Development* **137**:2807–2817

23. Huang A.H., Lu H.H., Schweitzer R. (2015) **Molecular regulation of tendon cell fate during development** *Journal of Orthopaedic Research* **33**:800–812

24. Tani S., Chung U.-i., Ohba S., Hojo H. (2020) **Understanding paraxial mesoderm development and sclerotome specification for skeletal repair** *Experimental & Molecular Medicine* **52**:1166–1177

25. Loh K.M., Chen A., Koh P.W., Deng T.Z., Sinha R., Tsai J.M., Barkal A.A., Shen K.Y., Jain R., Morganti R.M. (2016) **Mapping the pairwise choices leading from pluripotency to human bone, heart, and other mesoderm cell types** *Cell* **166**:451–467

26. Nakajima T., Shibata M., Nishio M., Nagata S., Alev C., Sakurai H., Toguchida J., Ikeya M. (2018) **Modeling human somite development and fibrodysplasia ossificans progressiva with induced pluripotent stem cells** *Development* **145**

27. Nakajima T., Nakahata A., Yamada N., Yoshizawa K., Kato T.M., Iwasaki M., Zhao C., Kuroki H., Ikeya M. (2021) **Grafting of iPS cell-derived tenocytes promotes motor function recovery after Achilles tendon rupture** *Nature communications* **12**:1–12

28. Gentsch G., Monteiro R., Smith J. (2017) **Cooperation between T-Box factors regulates the continuous segregation of germ layers during vertebrate embryogenesis** *Current topics in developmental biology* **122**:117–159

29. Harvey T., Flamenco S., Fan C.-M. (2019) **A Tppp3+ Pdgfra+ tendon stem cell population contributes to regeneration and reveals a shared role for PDGF signalling in regeneration and fibrosis** *Nature cell biology* **21**:1490–1503

30. Shukunami C., Takimoto A., Nishizaki Y., Yoshimoto Y., Tanaka S., Miura S., Watanabe H., Sakuma T., Yamamoto T., Kondoh G (2018) **Scleraxis is a transcriptional activator that regulates the expression of Tenomodulin, a marker of mature tenocytes and ligamentocytes** *Scientific reports* **8**:1–17

31. Liu H., Zhu S., Zhang C., Lu P., Hu J., Yin Z., Ma Y., Chen X., OuYang H. (2014) **Crucial transcription factors in tendon development and differentiation: their potential for tendon regeneration** *Cell and tissue research* **356**:287–298

32. Takahashi K., Yamanaka S. (2006) **Induction of pluripotent stem cells from mouse embryonic and adult fibroblast cultures by defined factors** *cell* **126**:663–676

33. Yamaguchi T.P., Takada S., Yoshikawa Y., Wu N., McMahon A.P. (1999) **T (Brachyury) is a direct target of Wnt3a during paraxial mesoderm specification** *Genes & development* **13**:3185–3190

34. Dunkman A.A., Buckley M.R., Mienaltowski M.J., Adams S.M., Thomas S.J., Satchell L., Kumar A., Pathmanathan L., Beason D.P., Iozzo R.V. (2014) **The tendon injury response is influenced by decorin and biglycan** *Annals of biomedical engineering* **42**:619–630

35. Hofmann M., Schuster-Gossler K., Watabe-Rudolph M., Aulehla A., Herrmann B.G., Gossler A. (2004) **WNT signaling, in synergy with T/TBX6, controls Notch signaling by regulating Dll1 expression in the presomitic mesoderm of mouse embryos** *Genes & development* **18**:2712–2717

36. Ishii M., Arias A.C., Liu L., Chen Y.-B., Bronner M.E., Maxson R.E. (2012) **A stable cranial neural crest cell line from mouse** *Stem cells and development* **21**:3069–3080

37. Lin H.-H., Bell E., Uwanogho D., Perfect L.W., Noristani H., Bates T.J., Snetkov V., Price J., Sun Y.-M. (2010) **Neuronatin promotes neural lineage in ESCs via Ca2+ signaling** *Stem Cells* **28**:1950–1960

38. Zhao X., van Praag H. (2020) **Steps towards standardized quantification of adult neurogenesis** *Nature Communications* **11**

39. Yao J.-j, Zhao Q.-r, Lu J.-m, Mei Y.-a. (2018) **Functions and the related signaling pathways of the neurotrophic factor neuritin** *Acta Pharmacologica Sinica* **39**:1414–1420

40. Berg D.A., Su Y., Jimenez-Cyrus D., Patel A., Huang N., Morizet D., Lee S., Shah R., Ringeling F.R., Jain R. (2019) **A common embryonic origin of stem cells drives developmental and adult neurogenesis** *Cell* **177**:654–668

41. Park D.S., Seo J.H., Hong M., Bang W., Han J.K., Choi S.C. (2013) **Role of Sp5 as an essential early regulator of neural crest specification in xenopus** *Developmental Dynamics* **242**:1382–1394

42. Shi J., Severson C., Yang J., Wedlich D., Klymkowsky M.W. (2011) **Snail2 controls mesodermal BMP/Wnt induction of neural crest** *Development* **138**:3135–3145

43. Dehmelt L., Halpain S. (2005) **The MAP2/Tau family of microtubule-associated proteins** *Genome biology* **6**:1–10

44. Simões-Costa M., Bronner M.E. (2015) **Establishing neural crest identity: a gene regulatory recipe** *Development* **142**:242–257

45. Deak K.L., Boyles A.L., Etchevers H.C., Melvin E.C., Siegel D.G., Graham F.L., Slifer S.H., Enterline D.S., George T.M., Vekemans M. (2005) **SNPs in the neural cell adhesion molecule 1 gene (NCAM1) may be associated with human neural tube defects** *Human genetics* **117**:133–142

46. Teppner I., Becker S., de Angelis M.H., Gossler A., Beckers J. (2007) **Compartmentalised expression of Delta-like 1 in epithelial somites is required for the formation of intervertebral joints** *BMC Developmental Biology* **7**:1–12

47. LeBlanc L., Kim M., Kambhampati A., Son A.J., Ramirez N., Kim J. (2022) **β-catenin links cell seeding density to global gene expression during mouse embryonic stem cell differentiation** *Iscience* **25**

48. Wu J., Fan Y., Tzanakakis E.S. (2015) **Increased culture density is linked to decelerated proliferation, prolonged G1 phase, and enhanced propensity for differentiation of self-renewing human pluripotent stem cells** *Stem cells and development* **24**:892–903

49. Kahane N., Kalcheim C. (2020) **Neural tube development depends on notochord-derived sonic hedgehog released into the sclerotome** *Development* **147**

50. Piacentino M.L., Bronner M.E. (2018) **Intracellular attenuation of BMP signaling via CKIP-1/Smurf1 is essential during neural crest induction** *PLoS Biology* **16**

51. Wymeersch F.J., Wilson V., Tsakiridis A. (2021) **Understanding axial progenitor biology in vivo and in vitro** *Development* **148**

52. Christ B., Huang R., Scaal M. (2004) **Formation and differentiation of the avian sclerotome** *Anatomy and embryology* **208**:333–350

53. Kult S., Olender T., Osterwalder M., Markman S., Leshkowitz D., Krief S., Blecher-Gonen R., Ben-Moshe S., Farack L., Keren-Shaul H. (2021) **Bi-fated tendon-to-bone attachment cells are regulated by shared enhancers and KLF transcription factors** *Elife* **10**

54. Blitz E., Sharir A., Akiyama H., Zelzer E. (2013) **Tendon-bone attachment unit is formed modularly by a distinct pool of Scx-and Sox9-positive progenitors** *Development* **140**:2680–2690

55. Sugimoto Y., Takimoto A., Akiyama H., Kist R., Scherer G., Nakamura T., Hiraki Y., Shukunami C. (2013) **Scx+/Sox9+ progenitors contribute to the establishment of the junction between cartilage and tendon/ligament** *Development* **140**:2280–2288

56. Miyabara S., Yuda Y., Kasashima Y., Kuwano A., Arai K. (2014) **Regulation of Tenomodulin Expression Via Wnt/beta-catenin Signaling in Equine Bone Marrow-derived Mesenchymal Stem Cells** *J Equine Sci* **25**:7–13 https://doi.org/10.1294/jes.25.7

57. Kishimoto Y., Ohkawara B., Sakai T., Ito M., Masuda A., Ishiguro N., Shukunami C., Docheva D., Ohno K. (2017) **Wnt/beta-catenin signaling suppresses expressions of Scx, Mkx, and Tnmd in tendon-derived cells** *PLoS One* **12** https://doi.org/10.1371/journal.pone.0182051

58. Lara H., Li Z., Abels E., Aeffner F., Bui M.M., ElGabry E.A., Kozlowski C., Montalto M.C., Parwani A.V., Zarella M.D. (2021) **Quantitative image analysis for tissue biomarker use: a white paper from the digital pathology association** *Applied Immunohistochemistry & Molecular Morphology* **29**

59. Schmittgen T.D., Livak K.J. (2008) **Analyzing real-time PCR data by the comparative C(T) method** *Nat Protoc* **3**:1101–1108 https://doi.org/10.1038/nprot.2008.73

60. Jiang W., Glaeser J.D., Salehi K., Kaneda G., Mathkar P., Wagner A., Ho R., Sheyn D. (2022) **Single-cell atlas unveils cellular heterogeneity and novel markers in human neonatal and adult intervertebral discs** *iScience* **25** https://doi.org/10.1016/j.isci.2022.104504

Author information

Angela Papalamprou

Orthopaedic Stem Cell Research Laboratory, Cedars-Sinai Medical Center, Los Angeles, United States, Board of Governors Regenerative Medicine Institute, Cedars-Sinai Medical Center, Los Angeles, United States, Department of Biomedical Sciences, Cedars-Sinai Medical Center, Los Angeles, United States

Victoria Yu

Orthopaedic Stem Cell Research Laboratory, Cedars-Sinai Medical Center, Los Angeles, United States, Board of Governors Regenerative Medicine Institute, Cedars-Sinai Medical Center, Los Angeles, United States, Department of Biomedical Sciences, Cedars-Sinai Medical Center, Los Angeles, United States

Wensen Jiang

Orthopaedic Stem Cell Research Laboratory, Cedars-Sinai Medical Center, Los Angeles, United States, Board of Governors Regenerative Medicine Institute, Cedars-Sinai Medical Center, Los Angeles, United States, Department of Biomedical Sciences, Cedars-Sinai Medical Center, Los Angeles, United States

Julia Sheyn

Orthopaedic Stem Cell Research Laboratory, Cedars-Sinai Medical Center, Los Angeles, United States, Board of Governors Regenerative Medicine Institute, Cedars-Sinai Medical Center, Los Angeles, United States, Department of Biomedical Sciences, Cedars-Sinai Medical Center, Los Angeles, United States

Tina Stefanovic

Orthopaedic Stem Cell Research Laboratory, Cedars-Sinai Medical Center, Los Angeles, United States, Board of Governors Regenerative Medicine Institute, Cedars-Sinai Medical Center, Los

Angeles, United States, Department of Biomedical Sciences, Cedars-Sinai Medical Center, Los Angeles, United States

Angel Chen
Orthopaedic Stem Cell Research Laboratory, Cedars-Sinai Medical Center, Los Angeles, United States, Board of Governors Regenerative Medicine Institute, Cedars-Sinai Medical Center, Los Angeles, United States, Department of Biomedical Sciences, Cedars-Sinai Medical Center, Los Angeles, United States

Chloe Castaneda
Orthopaedic Stem Cell Research Laboratory, Cedars-Sinai Medical Center, Los Angeles, United States, Board of Governors Regenerative Medicine Institute, Cedars-Sinai Medical Center, Los Angeles, United States, Department of Biomedical Sciences, Cedars-Sinai Medical Center, Los Angeles, United States

Melissa Chavez
Orthopaedic Stem Cell Research Laboratory, Cedars-Sinai Medical Center, Los Angeles, United States, Board of Governors Regenerative Medicine Institute, Cedars-Sinai Medical Center, Los Angeles, United States, Department of Biomedical Sciences, Cedars-Sinai Medical Center, Los Angeles, United States

Dmitriy Sheyn
Orthopaedic Stem Cell Research Laboratory, Cedars-Sinai Medical Center, Los Angeles, United States, Board of Governors Regenerative Medicine Institute, Cedars-Sinai Medical Center, Los Angeles, United States, Department of Orthopedics, Cedars-Sinai Medical Center, Los Angeles, United States, Department of Surgery, Cedars-Sinai Medical Center, Los Angeles, United States, Department of Biomedical Sciences, Cedars-Sinai Medical Center, Los Angeles, United States
ORCID iD: 0000-0002-3333-1485

For correspondence: Dmitriy.Sheyn@csmc.edu

Editors

Reviewing Editor
Kihyun Lee
Ewha Womans University, Seoul, Korea, the Republic of

Senior Editor
Murim Choi
Seoul National University, Seoul, Korea, the Republic of

Reviewer #1 (Public review):

Papalamprou et al. established a methodology to differentiate iPSCs to the syndetome stage and validated it by marker gene expression and scRNA-seq analysis. They further found that inhibition of WNT signaling enhanced the homogeneity of the cell population after identifying a group of branching-off cells that overexpressed WNT. Their results will be helpful in developing cell therapy systems for tendon injuries. However, there are several issues to improve the manuscript:

IPA analysis was performed after scRNA-seq. Although it is knowledge-based software with convenient graphic utilities, it is questionable whether an unbiased genome-level analysis was performed. Therefore, it is not convincing if WNT is the only and best signal for the

branching-off marker. Perhaps independent approaches, such as GO, pathway, or module analyses, should be performed to validate the findings.

According to the method section, two iPSC lines were used for the study. However, throughout the manuscript, it is not clearly described which line was used for which experiment. Did they show similar efficiency in differentiation and in responses to WNTi? It is also worrisome if using only two lines is the norm in the stem cell field. Please provide a rationale for using only two lines, which will restrict the observation of individual-specific differential responses throughout the study.

How similar are syndetome cells with or without WNTi? It would be interesting to check if there are major DEGs that differentiate these two groups of cells.

Please discuss the improvement of the current study compared to previous ones (e.g., PMID 36203346, 35083031, 35372337).

https://doi.org/10.7554/eLife.89652.2.sa3

Reviewer #2 (Public review):

Summary:

Dr. Sheyn and colleagues report the step-wise induction of syndetome-like cells from human induced pluripotent stem cells (iPSCs), following a previously published protocol which they adjusted. The progression of the cells through each stage, i.e. presomitic mesoderm (PSM), somitic mesoderm (SM), sclerotome (SCL), and syndetome (SYN)) is characterized using FACS, RT-qPCR and immunofluorescence staining (IF). The authors performed also single-cell RNA sequencing (scRNAseq) analysis of their step-wise induced cells and identify signaling pathways which are potentially involved in and possibly necessary for syndetome induction. They then optimized their protocol by simultaneous inhibition of BMP and Wnt signaling pathways, which lead to an increase in syndetome induction while inhibiting off target differentiation into neural lineages.

Strengths:

The authors conducted scRNAseq analysis of each step of their protocol from iPSCs to syndetome-like cells and employed pathway analysis to uncover further insights into somitic mesoderm (SM) and syndetome (SYN) differentiation. They found that BMP inhibition, in conjunction with the inhibition of WNT signaling, plays a role in driving syndetome differentiation. Analyzing their scRNAseq results, they could improve the syndetome induction efficiency of their protocol from 47.6% to 67%-78% while off-target differentiation into neural lineages could be reduced.

Weaknesses:

The authors demonstrated the efficiency of syndetome induction solely by scRNA-seq data analysis before and after pathway inhibition, without using e.g. FACS analysis or immunofluorescence (IF)-staining based assessment. A functional assessment and validation of the induced cells is also completely missing.

https://doi.org/10.7554/eLife.89652.2.sa2

Reviewer #3 (Public review):

Papalamprou et al sought to fine tune existing tenogenic differentiation protocols to develop a robust multi-step differentiation protocol to induce tendon cells from human GMP-ready iPSCs. In so doing, they found that while existing protocols are capable of driving cells towards a syndetome-like fate, the resultant cultures contain highly heterogeneous cell populations with sub-optimal cell survival. Through single cell transcriptomic analysis they identify WNT signaling as a potential driver of an off-target neural population and show that inhibition of WNT signaling at the later 2 stages of differentiation can be used to promote higher efficiency of generation of syndetome-like cells.

This paper includes a useful paradigm for identifying transcriptional modulators of cell fate during differentiation and a clear example where transcriptional data can be used to guide the chemical modulation of a differentiation protocol to improve cell output. The paper's conclusions are mostly well supported by the data, but the image analysis and discussion need to be improved to strengthen the impact.

The data outlining the differences between the differentiation outcome of the two tested iPSCs is intriguing, but the authors fail to comment on potential differences between the two iPSC lines that could result in drastically different cell outputs from the same differentiation protocol. This is a critically important point, as the majority of the SCX+ cells generated from the 007i cells using their WNTi protocol were found in the FC subpopulation that failed to form from the 83i line under the same protocol. From the analysis of only these 2 cells lines in vitro, it is difficult to assess whether this WNTi protocol can be broadly used across multiple cell lines to generate tenogenic cells. The authors failed to update the text of the manuscript to reflect the potential differences in the two cell lines and the general applicability of their protocol, but rather just include the description of the proposed explanation in the response to reviewer comments. These critical differences in the response to their protocol and their implications for the applications of this proof-of-concept study should be included in the main text.

The authors make claims about changes in protein expression but fail to quantify either fluorescence intensity or percent cell expression from their immunofluorescence analyses to substantiate these claims. The authors state in their response to reviewers that immunofluorescence is qualitative but continue to make quantitative statements such as upregulated or downregulated in both the text and legend describing these images. The authors should either perform the quantification of the IFs, use Western blots for protein quantification of their cell cultures, use Flow Cytometry to count cell numbers, or remove these quantitative words from the description of the images. The image quality and staining specificity continue to be a limitation of this study. These claims are not fully supported by the data as presented as it is unclear whether there is increased expression of tendon markers at the protein level or more cells surviving the protocol.

https://doi.org/10.7554/eLife.89652.2.sa1

Author response:

The following is the authors' response to the original reviews.

> ***Reviewer 1:***
>
> *Comment 1: IPA analysis was performed after scRNA-seq. Although it is knowledge-based software with convenient graphic utilities, it is questionable whether an unbiased genome-level analysis was performed. Therefore, it is not convincing if WNT is the only*

> *and best signal for the branching-off marker. Perhaps independent approaches, such as GO, pathway, or module analyses, should be performed to validate the finding.*

Thanks for your comment. We agree with the reviewer that IPA is a knowledge-based and a hypothesis-driven method. Our hypothesis was that WNT/BMP pathways, among others, are heavily involved in the development of mesenchymal tissues in general and differentiation of tendons specifically. Therefore, we have looked at differentially expressed genes between clusters from a broad array of pathways featured in IPA that could point us towards molecular function that could make a difference. We further corroborated this hypothesis by using WNT inhibitors in subsequent experiments. To address this point, we have supplemented the discussion section with the following remark:

"This study is not without limitations. The IPA network analysis is a knowledge-based and hypothesis driven platform. We have specifically targeted known pathways to be involved in syndetome differentiation. However, WNT signaling stood out with very specific affinity to the off-target populations and we have verified our findings with experiments proving this hypothesis."

Per the reviewer's suggestion, we also performed a non-biased GO analysis (Supp. Fig. 6). Multiple pathways were detected in the three clusters of interest (Supp. Fig. 6A-C), including integrin-related and TGFβ-related pathways. However, in these three clusters of interest, WNT signaling was also detected as a prominent pathway. Therefore, we could conclude that it plays a pivotal role in the differentiation process. This hypothesis was later corroborated with WNT inhibitor experiments.

> *Comment 2: According to the method section, two iPSC lines were used for the study. However, throughout the manuscript, it is not clearly described which line was used for which experiment. Did they show similar efficiency in differentiation and in responses to WNTi? It is also worrisome if using only two lines is the norm in the stem cell field. Please provide a rationale for using only two lines, which will restrict the observation of individual-specific differential responses throughout the study.*

Thanks for your comment. This proof-of-concept study is the first investigation that compares data of an in vitro tenogenic induction protocol that has been tested in more than one human iPSC lines. We agree that line-specific phenomena are difficult to interpret and reproduce. Therefore, it is critical to provide data supporting that the findings can be reproduced in more than one line. Some early studies used one line as proof of concept, however now we realize the need to show that the protocol works in at least one additional line.

Here we used the GMP-ready iPSC line CS0007iCTR-n5 for all optimization experiments. This newer low passage feeder-free line was generated from PBMCs and was designated as GMP-ready in the manuscript because it has been derived and cultured using cGMP xeno-free components (mTESR plus medium and rhLaminin-521 matrix substrate instead of Matrigel). We then wanted to confirm the application of the optimized protocol using the reference control line CS83iCTR-22n1 which has already been more widely used by our group1-5 and others.6 This line has been derived from fibroblasts and has been grown and expanded using MatrigelTM and mTESR1, followed by mTESR plus media.

The question of number of lines needed is stage-dependent. In our opinion at the proof-of-concept level, two lines, one of which has been generated in GMP-like conditions is sufficient. Confirmation with multiple lines becomes more pertinent as we move towards scale-up/manufacturing, where considerations regarding robustness and consistency are raised. However, at this stage, it is crucial to understand the developmental processes that are involved in cell differentiation to ensure a more robust protocol can be modified and adapted later. In future studies, as we move towards clinical translation, it is warranted that the

approach presented in this work will be further optimized and subsequently evaluated using at least 3 different cell lines that have been generated from various sources.

> *Comment 3: How similar are syndetome cells with or without WNTi? It would be interesting to check if there are major DEGs that differentiate these two groups of cells.*

Thanks for your comment. Single cell RNAseq analysis revealed that treatment with WNTi upregulated tenogenic markers. In SYNWNTi, the expression levels of stage-specific markers COL1A1, COL3A1, SCX, MKX, DCN, BGN, FN1, and TNMD were higher compared to the untreated SYN group, as shown in Figure 5C. Density plots depicted an increase in the number of cells expressing COL1A1, COL3A1, SCX and TNMD in SYNWNTi compared to the SYN group, as illustrated in Figure 5D. Trajectory analysis of the WNTi-treated group revealed the absence of bifurcations observed in the untreated group (Fig. 5E). Therefore, it can be conjured that syndetome cells with and without WNTi are different.

> *Comment 4: Please discuss the improvement of the current study compared to previous ones (e.g., PMID 36203346 my study, 35083031- Tsutsumi, 35372337- Yoshimoto).*

Thanks for your comment. In Papalamprou et al (2023)3, we differentiated iPSCs to mesenchymal stromal-like cells (iMSCs), which were then cultured into a 2D dynamic bioreactor for 7 days. In that study, we examined the impact of simultaneous overexpression of the tendon transcription factor Scleraxis (SCX) using a lentiviral vector and mechanical stimulation on the process of tenogenic differentiation. Following 7 days of uniaxial cyclic loading, we observed notable modifications in the morphology and cytoskeleton organization of iPSC-derived MSCs (iMSCs) overexpressing SCX. Additionally, there was an increase in extracellular matrix (ECM) deposition and alignment, along with upregulation of early and late tendon markers. This proof-of-concept study showed that iPSC-derived MSCs could be a viable cell candidate for cell therapy applications and that mechanical stimulation is contributing to the differentiation of iMSCs towards the tenogenic lineage.

Similarly, Tsutsumi et al7 overexpressed the tendon transcription factor Mohawk (MKX) stably in iPSC-derived MSCs using lentiviral vectors. These cells were then used to seed collagen hydrogels which were mechanically stimulated in a cyclic stretch 3D culture bioreactor for 15 days to create artificial tendon-like tissues, which the authors termed “bio-tendons”. Bio-tendons were then decellularized to remove cellular remnants from the xenogeneic human iPSC-derived cells and were subsequently transplanted in an in vivo Achilles tendon rupture mouse model. The authors reported improved histological and biomechanical properties in the Mkx-bio-tendon mice vs. the GFP-bio-tendon controls, providing another proof-of-concept study in favor of the utilization of iPSC-derived MSCs for tendon cell therapies, while also addressing the immunogenicity of cells of allogeneic/xenogeneic origin. Therefore, the above two studies used tendon transcription factor overexpression and mechanical loading either in 2D or 3D to differentiate MSCs towards the tendon/ligament lineage.

Yoshimoto et al8 optimized a stepwise iPSC to tenocyte induction protocol using a SCX-GFP transgenic mouse iPSC line, by monitoring GFP expression over time. The group performed scRNA-seq to characterize the induction of mesodermal progenitors towards the tenogenic lineage and to shed light into their developmental trajectory. That study unveiled that Retinoic Acid (RA) signaling activation enhanced chondrogenic differentiation, which was in contrast to the study of Kaji et al (2021), which also used a SCX-GFP mouse iPSC line. Kaji et al inhibited TGF and BMP signaling during the process of mesodermal induction and reported that RA signaling eliminated SCX induction entirely and promoted a switch to neural fate. Yoshimoto et al suggested that variations in mesodermal cell identity could be due to the different methods used for mesodermal differentiation. In contrast to the Kaji et al study, Yoshimoto et al opted to stimulate WNT and block the Hedgehog pathway during mesoderm

induction. Loh et al (2016) identified the branchpoint from the primitive streak to either the paraxial mesoderm (PSM) or the lateral plate mesoderm (LPM) as the result of two mutually exclusive signaling conditions. Specifically, they reported that induction of PSM was achieved through BMP suppression and WNT stimulation, while the specification of lateral mesoderm was accomplished by BMP stimulation and WNT suppression, all with concurrent TGFβ suppression/FGF stimulation. Lastly, a similar approach towards PSM induction from primitive streak (TGF off/BMP off/ WNT on/FGF on) has been used by many subsequent studies Matsuda et al (2020),9 Wu et al (2021)10 and Nakajima et al (2021).11 The diversity of the above-mentioned approaches points to the plasticity of mesodermal progenitors and the need for additional studies to better understand mesodermal specification and subsequent induction towards sclerotome and syndetome.

In the current study we optimized a stepwise differentiation protocol using xeno-free cGMP ready media and two different cell lines, one of which was cGMP-ready. We used scRNA-seq to characterize the differentiation, which led us to identify off-target cells that were closer to a neural phenotype. We performed pathway analyses and hypothesized that WNT signaling activity might have contributed to the emergence of the off-target cells. To test this, we used a WNT inhibitor (PORCN) to block WNT activity at the SCL stage and at the SYN stage. We found that blockade of WNT signaling at the end of the SM stage and during SCL and SYN induction resulted in a more homogeneous population, while eliminating the neural-like cell cluster. This is the first study that utilized scRNA-seq to shed light into the developmental trajectory of stepwise iPSC to tendon differentiation of human iPSCs and provided a proof-of-concept for the generation of a more homogeneous syndetome population. Further studies are needed to further fine-tune both the process and the final product, as well as elucidate the functionality of iPSC-derived syndetome cells in vitro and in vivo.

> ***Reviewer 2:***
>
> *General concerns: The authors demonstrated the efficiency of syndetome induction solely by scRNA-seq data analysis before and after pathway inhibition, without using e.g. FACS analysis or immunofluorescence (IF)-staining based assessment. A functional assessment and validation of the induced cells is also completely missing.*

We appreciate and agree with the reviewer's critique regarding further analyses of differentiated iPSC-derived syndetome-like cells, including functional assessment of the differentiated cells. Immunofluorescence was used at all timepoints of induction for phenotype confirmation (Fig. 2,4). Flow cytometry for DLL1 was utilized to benchmark efficient differentiation to PSM (Loh et al,12 Nakajima et al11. Specifically, DLL1 expression was assessed with flow cytometry after 4 days of induction, and was used to optimize the parameter of initial iPSC aggregate seeding density, which has been previously found to be crucial for in vitro differentiation protocols (Loh et al12). Unfortunately, this parameter is usually not reported although it could be critical to establish protocol replication between different lines.

The function of tendon progenitors is usually reported as response to mechanical cues and the ability to regenerate tendon injuries. In future studies we intend to assess the functionality of the generated syndetome and tendon progenitors and their response to in vitro biomechanical stimulation as previously reported to iMSCSCX+ cells3, 13 and in vivo in a critical tendon defect similarly to what has been previously reported.2

> *Comment 1: Notably, in Figure 1D, certain PSM markers (TBXT, MSGN1, WNT3A) show higher expression on day 3. If the authors initiate SM induction on day 3 instead of day 4, could this potentially enhance the efficiency of syndetome-like cell induction?*

Thanks for your comment. In the current work, we initially optimized differentiation to PSM via expression of DLL1, whose gene expression peaked at d4. We found that this was influenced by the initial iPSC aggregate seeding density. We wanted to generate a homogeneous DLL1+ population which we assessed via gene expression, flow cytometry, IF and scRNA-seq (Fig. 1D, 2C, 3C and Suppl. Fig.1). Given the fact that different lines might display a diverse developmental timeline, we also confirmed reproducibility of the protocol with a second cell line. We appreciate the reviewer's suggestion to investigate additional protocol iterations, such as the proposed one at the PSM stage, as we move towards a better understanding of key developmental events during in vitro induction.

> *Comment 2: In the third paragraph of the result section the authors note, "Interestingly, SCX, a prominent tenogenic transcription factor, was significantly downregulated at the SCL stage compared to iPSC, but upregulated during the differentiation from SCL to SYN." Despite this increase, the expression level of SCX in SYN remains lower than that in iPSCs in Fig.1G and Fig.3C. Can the authors provide an explanation for this? Can the authors provide IF data using iPSCs and compare it with in vitro-induced SYN cells? Can the authors provide e.g. additional scRNA-seq data which could support this statement?*

Thank you for your comment. In Fig. 1G, SCX expression in SYN was upregulated compared to SCL, however, it was shown to be similar to iPSCs. This suggests a baseline stochastic expression of SCX possibly stemming from spontaneous differentiation of iPSCs in culture (Fig. 3C). Previous research has shown that tenogenic marker gene expression tends to reduce during postnatal tendon maturation (Yin et al., 2016b14 Grinstein et al., 2019.15 Yoshimoto et al (2022) utilized a transgenic mouse iPSC-SCX-GFP line to track SCX expression. It was shown that SCX expression peaked after 7d of tenogenic induction and was then decreased at day 14, which marked the end of tenogenic induction. The authors postulated that this pattern of gene expression could either indicate further maturation of tenocytes at subsequent time points, or that the number of non-tenogenic cells increased from T7 to T14.

In the present work, we showed SCX gene expression upregulation in SYN compared to SCL, as well as significant upregulation of TNMD, EGR1, COL1A1 and COL3A1 (Fig.1G). Supp. Fig.8 has been added to show feature plots of SCX and TNMD expression from SCL, SYN and SYNWNTi. The significant upregulation of later markers of tenogenic differentiation suggests that the 21 days of tenogenic induction might have matured the cells. Since gene expression analysis only conveys a snapshot of the transcriptional profile of a cell population, it is likely that we might have missed the peak of SCX upregulation (Supp. Fig. 5). Following treatment with the WNT inhibitor, the SYNWNTi group displayed increased SCX expression (% cells expressing SCX) compared to SYN, which might also be due to a more homogeneous population of syndetome-like cells following treatment with WNTi. In the SYNWNTi group, TNMD was shown to be expressed in the SYN cluster, whereas SCX was mostly found in the cluster that was labelled as fibrocartilage (FC) cluster based on the expression of COL2A1/SOX9/FN1/BGN/COL1A1 markers. Due to the fact that SCX+/SOX9+ progenitor cells are able to give rise to both tendon and cartilage (Sugimoto 2013)16, it could be postulated that this cluster contains tendon progenitors. Interestingly, the FC cluster was not observed in the second iPSC line that we tested, which resulted in a more homogeneous induction to syndetome (78.5% vs. 66.9% SYN cells, Supp. Table 1 & Supp. Fig.3). This slight discrepancy between the two lines and more specifically the presence of the FC cluster only in the 007i line, warrants further investigation. Taken together, these data indicate that the tenogenic induction duration could likely be shortened. Further work to assess the time course of SCX expression over the entire tenogenic induction could be used to further optimize the in vitro induction. For instance, a human edited iPSCSCX-GFP+ line could be generated and used to track SCX expression during the entire induction.

> *Comment 3: In the fourth paragraph of the result section the authors state, "SM markers (MEOX1, PAX3) and SCL markers (PAX1, PAX9, NKX3.2, SOX9) were upregulated in a stepwise manner." However, the data for MEOX1 and NKX3.2 seems to be missing from Figure 3B-C. The authors should provide this data and/or additional support for their claim.*

Thanks for your comment. Feature plots for MEOX1 and NKX3.2 have been added to the Supplemental information (Supp. Fig. 9).

> *Comment 4: In Figures 2B and 2E, the background of the red channel seems extremely high. Are there better images available, particularly for MEOX1? Given the expected high expression of MEOX1 in SM cells, the authors should observe a strong signal in the nucleus of the stained somitic mesoderm-like cells, but that is not the case in the shown figure. The authors should provide separate channel images instead of merged ones for clarity. The antibody which the authors used might not be specific. Can the authors provide images using an antibody which has been shown to work previously e.g. antibody by ATLAS (Cat#: HPA045214)?*

As requested by the reviewer, we have provided separate channels for those images in the Supplement (Supp. Fig. 7). The images show relatively high expression of these markers in SM cells.

> *Comment 5: In Fig. 2C and Supplementary Fig. 1, the authors present data from immunofluorescence (IF) staining and FACS analysis using a DLL1 antibody. While FACS analysis indicates an efficiency of 96.2% for DLL1+ cells, this was not clearly observed in their IF data. How can the authors explain this discrepancy? Could the authors quantify their IF data and compare it with the corresponding FACS data?*

Thanks for your comment. We performed flow cytometric analysis of DLL1 expression to optimize cell seeding density using the 007i line. In the present study, we used IF only in a qualitative manner, that is to confirm protein expression of selected markers. It could be noted that the use of poly-lysine coated coverslips, which are needed for IF, might have slightly altered the density of the cells on the coverslip vs. the plate. Lastly, it cannot be ruled out that the different substrate could have influenced their phenotype differentially through matrix interactions and signaling. On the other hand, flow cytometry by nature is a quantitative and single cell approach, whereas IF staining is qualitative. Therefore, for the purpose of this proof-of-concept work, we tend to trust the quantitative data from the flow cytometry results more than semi-quantitative confirmation achieved through IF staining using coverslips.

> *Comment 6: In Fig. 2G, PAX9 is expected to be expressed in the nucleus, but the shown IF staining does not appear to be localized to the nucleus. Could the authors provide improved or alternative images to clarify this? The authors should use antibodies shown to work with high specificity as already reported by other groups.*

Thanks for your comment. Indeed, the staining seems to be mostly cytoplasmic. We have used antibodies that were previously reported3 and repeated the staining, however, the same results were replicated. We can speculate that this transcription factor has additional role in the iPSC-derived cells and might be traveling to the cytoplasm. Unfortunately, we have no evidence to this phenomenon.

> *Comment 7: Why did the authors choose to display day 10 data for SYN induction in Fig. 4A? Could they provide information about the endpoint of their culture at day 21?*

Thank you for your comment. In Fig. 1G we provided gene expression analyses results for several selected early and later tendon markers for the endpoint of our culture, that is day 21. Following scRNA-seq at each stage of the differentiation (iPSC at d0, PSM at d4, SM at d8, SCL at d11 and the endpoint day 32 for SYN), we performed DEG analysis using the IPA platform. We identified activation of genes associated with the WNT signaling pathway in the off-target clusters. We hypothesized that WNT pathway inhibition might block the formation of unwanted fates and induce a more homogeneous differentiation outcome. We thus tested a WNT inhibitor and compared the inhibitor-treated group with a non-treated group. We then assessed selected neural markers during the course of the inhibitor application. In Fig. 4A we presented gene expression of key selected markers at day 21 using qPCR, which was approximately in the middle of the syndetome induction. Since we observed that the inhibitor downregulated the selected neural markers, we then applied the inhibitor until the endpoint of the initial induction and proceeded to analyze the results using scRNA-seq (Fig. 5). Lastly, it should be acknowledged that this was a proof-of-concept study, and additional optimizations are needed regarding the application of the inhibitor (timing, duration, concentration, etc).

> *Comment 8: In Supplementary Fig. 5, the authors depicted the expression level of SCX, a SYN marker, which peaked at day 14 and then decreased. By day 21, it reached a level comparable to that of iPSCs. Given this observation, could the authors provide a characterization of the cells at day 21 during SYN induction using IF? What was the rationale behind selecting 21 days for SYN induction? The authors also need to show 'n numbers'; how many times were the experiments repeated independently (independent experiments)?*

Thanks for your comment. During the optimization process, we initially used RT-qPCR to track gene expression of selected tenogenic markers using the 007i line. We found that after 21 days of tenogenic induction there was upregulation of the few established tendon markers, that is COL1A1, COL3A1, EGR1 and quite importantly, the more definitive later tendon marker, TNMD. Thus, we decided to proceed with this protocol prior to testing other compounds including the WNT inhibitor WNT-C59. However, as has been discussed in the manuscript, this extended tenogenic induction resulted in cell attrition without the application of the WNT inhibitor. This phenomenon was ameliorated following WNT inhibition. Thus, it could be postulated that the protocol could be further optimized by shortening tenogenic induction to less than 21 days.

The experiments that were conducted to optimize the differentiation process were repeated independently at least n=3 times using qPCR and IF using two lines, that is the 007i and the 83i line as described in the manuscript. The scRNAseq analysis represents a population of cells from in vitro differentiation that originated from the same donor line, therefore it was performed on n=1 sample at each stage. However, the effects of inhibitor application (sample SYNWNTi) were also confirmed using a second cell line (83i), thus a total of n=2 independent samples were analyzed.

> *Comment 9: Overall the shown immunofluorescence (IF) data does not appear convincing. Could the authors please provide clearer images, including separate channel images, a bright field image, and magnified views of each staining?*

Thanks for your comment. The separate channels images were added to the supplemental data (Supp. Fig. 7). We agree with the reviewer regarding the limitations of IF staining, especially with the added confounding factor of using poly-lysine coated coverslips. We would like to point out, that in the current work IF staining is not the main finding or the primary outcome measure, and that it is only used to further support the differentiation by providing a qualitative assessment of protein presence and localization. We describe in this

paper our thesis regarding the limitations of IF and the need for more high-throughput unbiased approaches to quantification when using IF staining. For instance, spatial transcriptomics combined with mass cytometry or flow cytometry could be used for a more unbiased approach. Thus, in the present manuscript we based our conclusion on the quantitative gene expression, single cell sequencing and flow cytometry.

> *Comment 10: As stated by the authors in the manuscript, another research group performed FACS analysis to assess the efficiency of syndetome induction using SCX antibody, and/or quantification of immunofluorescence (IF) with SCX, MKX, COL1A1, or COL2A1 antibodies. Could the authors conduct a comparative analysis of syndetome induction efficiency both before and after protocol optimization, utilizing FACS analysis in conjunction with an SCX reporter line or antibody staining, e.g. quantifying induction efficiency via immunofluorescence (IF) staining with syndetome-specific marker genes?*

Thank you for your comment. As discussed in a previous comment, we agree with the reviewer that the generation of a human iPSC-SCX-GFP line would shed light into SCX expression over the entire course of induction. In the current work we used IF as qualitative confirmation of specific marker expression and we showed the presence of SCX, MKX, COL1 and COL3 in SYNWNTi as well as the absence of neuronal markers. As we also pointed it out in the present manuscript, IF can only be considered as a semi-quantitative assessment burdened with several technical limitations as well as operator bias and lower sensitivity and accuracy compared to flow cytometry or scRNA-seq, unless performed in a more unbiased manner. To further clarify this point, firstly, using poly-lysine coated coverslips for IF staining, results in a different substrate environment compared to the Geltrex-coated plates that were used for the induction. Additionally, we noticed that cells grew overconfluent at the edges of the coverslips. This is an important point, since as we have observed in this work, seeding density is critical for the reproducibility of the protocol. It could further be postulated that a different cell substrate stiffness might also have an effect on this process. In our opinion, in this context IF should rather be used qualitatively and a combination of flow cytometry with scRNAseq should be utilized to draw quantitative conclusions such as induction efficiencies of a certain cell type. Since we also observed inconsistencies with the SCX antibodies we tested, the generation of edited human iPSC lines (such as SCX-GFP, MKX-GFP and TNMD-GFP) would be the preferred approach to further explore the efficiency of differentiation.

> *Comment 11: To enhance the paper's significance, the authors should conduct functional validation experiments and proper assessment of their induced syndetome-like cells. They could perform e.g. xeno-transplantation experiments with syndetome cells into SCID-mice or injury models. They could also assess whether the in vitro induced cells could be applied for in vitro tendon/ligament formation.*

Thanks for your comment. For the purpose of this proof-of-concept in vitro study, our primary goal was to initially evaluate a stepwise tenogenic induction protocol using GMP-ready cell lines and chemically defined media. Then, we wanted to utilize the analytical power of scRNA-seq in order to characterize and optimize the protocol, thus focusing on one developmental stage that is not well understood, that of syndetome specification from sclerotome, and hypothesized that by fine-tuning the WNT pathway we would be able to generate a more homogeneous syndetome cell population. We fully agree with the reviewer that the warranted next steps should be to conduct several functional validation experiments, such as in vitro 2D/3D tendon/ligament formation and in vivo transplantation in allogeneic or xenogeneic injury models.

> *Comment 12: The authors should also compare their scRNA-seq data with actual human embryo data sets, something which could be done given the recent increase in available*

> *human embryo scRNA-seq data sets.*

This is a great idea and intriguing study. Unfortunately, not all data sets are available at the moment and specifically embryonic and MSK scRNA-seq data is very scarce, although growing. We have no access to data sets from human tendon development, and thus will have to leave this comparison for future studies.

> ***Reviewer 3:***
>
> *Comment 1: The data outlining the differences between the differentiation outcome of the two tested iPSCs is intriguing, but the authors fail to comment on potential differences between the two iPSC lines that could result in drastically different cell outputs from the same differentiation protocol. This is a critically important point, as the majority of the SCX+ cells generated from the 007i cells using their WNTi protocol were found in the FC subpopulation that failed to form from the 83i line under the same protocol. From the analysis of only these 2 cell lines in vitro, it is difficult to assess whether this WNTi protocol can be broadly used to generate tenogenic cells.*

Thanks for your comment. This proof-of-concept study is the first investigation that compares data of an in vitro tenogenic induction protocol that has been tested into more than one cell lines. Using unsupervised clustering we identified 11 clusters, which were classified into 6 cell subpopulations. The only observed difference between the two lines was a small subset that was labeled as fibrocartilage (FC), which displayed expression of both tenogenic and chondrogenic markers. This subpopulation was observed in 007i line but not in the 83i line at the end of the SYN induction. Importantly, DEG analysis also showed that it was enriched for SCX. It has been shown that SCX+/SOX9+ progenitors are a distinct multipotent cell group, responsible for the development of SCX−/SOX9+ chondrocytes and SCX+/SOX9− tenocytes/ligamentocytes (Sugimoto 2013)16. As noted in a previous comment (Comment 2 from Reviewer 1), we might have missed SCX upregulation during the 21-day syndetome induction. This can be further supported by Fig. 5E trajectory analysis which shows that this subpopulation (FC) precedes the SYN cell subpopulation. The fact that this subpopulation was present in one line but not the other, might indicate that 83i line resulted in a more mature tendon population. Therefore, we would rather posit that in the case of 83i line, it might not be that the FC subpopulation failed to form, but rather that it was missed in our scRNAseq endpoint analysis which showed that a more homogeneous SYN population was formed (8.7 % in 007i vs. 0.26 % in 83i, Supp. Table 1 & Supp. Fig. 3B). Future studies are warranted to characterize the SYN induction timeline as it pertains to SCX expression followed up by maturation from tenogenic progenitor to tenocytes.

> *Comment 2: The authors make claims to changes in protein expression but fail to quantify either fluorescence intensity or percent cell expression from their immunofluorescence analyses to substantiate these claims. These claims are not fully supported by the data as presented as it is unclear whether there is increased expression of tendon markers at the protein level or more cells surviving the protocol. Additionally, in images where 3 channels are merged, it would be helpful to show individual channels where genes are shown in similar spectra (ie. Fig 2I SCX/MKX). Furthermore, the current layout and labelling scheme of Figure 4 makes it very difficult to compare conditions between SYN and SYNWNTi protocols.*

Thanks for your comment. Protein expression at each stage was verified with immunofluorescence cytochemistry whereby cells were cultured onto poly-lysine coated coverslips, which were then fixed, stained and imaged (Fig. 2). However, prior to WNT inhibitor application, we noticed gradual cell attrition in the cultures at the end of differentiation (Fig. 1B, 2I). The images show qualitative differences with and without the

WNT inhibitor. This could be attributed to the heterogeneity of the cell population at SCL stage, which was confirmed by scRNA-seq (Fig. 3A). As it has been discussed previously (Reviewer 2 comments 5 & 9), in the current paper we didn't provide any IF quantitative analysis because of the qualitative nature of the staining technique. In future work another high-resolution imaging modality will be considered like single cell proteomics and flow cytometry or mass cytometry in order to perform a more unbiased quantitative single cell analysis across different stages and samples. Furthermore, we have added single channel images in the supplemental information.

> *Comment 3: Individual data points should also be presented for all qPCR experiments (ie. Fig 4A). Biological replicate information is missing from several experiments, particularly the immunofluorescence data, and it is unclear whether the qPCR data was generated from technical or biological replicates.*

Thanks for your comment. We have added additional information regarding replicates in each figure legend. We have also changed Fig. 4A.

(1) Glaeser JD, Bao X, Kaneda G, et al. iPSC-neural crest derived cells embedded in 3D printable bio-ink promote cranial bone defect repair. Sci Rep. Nov 4 2022;12(1):18701. https://www.ncbi.nlm.nih.gov/pubmed/36333414

(2) Kaneda G, Chan JL, Castaneda CM, et al. iPSC-derived tenocytes seeded on microgrooved 3D printed scaffolds for Achilles tendon regeneration. J Orthop Res. Oct 2023;41(10):2205-2220. https://www.ncbi.nlm.nih.gov/pubmed/36961351

(3) Papalamprou A, Yu V, Chen A, et al. Directing iPSC differentiation into iTenocytes using combined scleraxis overexpression and cyclic loading. J Orthop Res. Jun 2023;41(6):1148-1161. https://www.ncbi.nlm.nih.gov/pubmed/36203346

(4) Sheyn D, Ben-David S, Tawackoli W, et al. Human iPSCs can be differentiated into notochordal cells that reduce intervertebral disc degeneration in a porcine model. Theranostics. 2019;9(25):7506-7524. https://www.ncbi.nlm.nih.gov/pubmed/31695783

(5) Später T, Kaneda G, Chavez M, et al. Retention of Human iPSC-Derived or Primary Cells Following Xenotransplantation into Rat Immune-Privileged Sites. Bioengineering. 2023;10(9):1049. https://www.mdpi.com/2306-5354/10/9/1049

(6) Sareen D, O'Rourke JG, Meera P, et al. Targeting RNA foci in iPSC-derived motor neurons from ALS patients with a C9ORF72 repeat expansion. Sci Transl Med. Oct 23 2013;5(208):208ra149. https://www.ncbi.nlm.nih.gov/pubmed/24154603

(7) Tsutsumi H, Kurimoto R, Nakamichi R, et al. Generation of a tendon-like tissue from human iPS cells. J Tissue Eng. Jan-Dec 2022;13:20417314221074018. https://www.ncbi.nlm.nih.gov/pubmed/35083031

(8) Yoshimoto Y, Uezumi A, Ikemoto-Uezumi M, et al. Tenogenic Induction From Induced Pluripotent Stem Cells Unveils the Trajectory Towards Tenocyte Differentiation. Front Cell Dev Biol. 2022;10:780038. https://www.ncbi.nlm.nih.gov/pubmed/35372337

(9) Matsuda M, Yamanaka Y, Uemura M, et al. Recapitulating the human segmentation clock with pluripotent stem cells. Nature. Apr 2020;580(7801):124-129. https://www.ncbi.nlm.nih.gov/pubmed/32238941

(10) Wu CL, Dicks A, Steward N, et al. Single cell transcriptomic analysis of human pluripotent stem cell chondrogenesis. Nat Commun. Jan 13 2021;12(1):362. https://www.ncbi.nlm.nih.gov/pubmed/33441552

(11) Nakajima T, Nakahata A, Yamada N, et al. Grafting of iPS cell-derived tenocytes promotes motor function recovery after Achilles tendon rupture. Nat Commun. Aug 18 2021;12(1):5012. https://www.ncbi.nlm.nih.gov/pubmed/34408142

(12) Loh KM, Chen A, Koh PW, et al. Mapping the Pairwise Choices Leading from Pluripotency to Human Bone, Heart, and Other Mesoderm Cell Types. Cell. Jul 14 2016;166(2):451-467. https://www.ncbi.nlm.nih.gov/pubmed/27419872

(13) Yu V, Papalamprou A, Sheyn D. Generation of Induced Pluripotent Stem Cell-Derived iTenocytes via Combined Scleraxis Overexpression and 2D Uniaxial Tension. JoVE. 2024/03/01 2024(205):e65837. https://app.jove.com/65837

(14) Yin Z, Hu JJ, Yang L, et al. Single-cell analysis reveals a nestin(+) tendon stem/progenitor cell population with strong tenogenic potentiality. Sci Adv. Nov 2016;2(11):e1600874. https://www.ncbi.nlm.nih.gov/pubmed/28138519

(15) Grinstein M, Dingwall HL, O'Connor LD, Zou K, Capellini TD, Galloway JL. A distinct transition from cell growth to physiological homeostasis in the tendon. Elife. Sep 19 2019;8. https://www.ncbi.nlm.nih.gov/pubmed/31535975

(16) Sugimoto Y, Takimoto A, Akiyama H, et al. Scx+/Sox9+ progenitors contribute to the establishment of the junction between cartilage and tendon/ligament. Development. Jun 2013;140(11):2280-2288. https://www.ncbi.nlm.nih.gov/pubmed/23615282

https://doi.org/10.7554/eLife.89652.2.sa0